

THERMODYNAMIC PROPERTIES OF EQUILIBRIUM AIR BY AN EXACT TWO-EQUATION MODEL FOR EULER AND NAVIER–STOKES CFD ALGORITHMS

JOE IANNELLI*

*Department of Mechanical & Aerospace Engineering and Engineering Science, The University of Tennessee,
315 Perkins Hall, Knoxville, TN 37996-2030, U.S.A.*

SUMMARY

This paper details an exact two-equation procedure to generate pressure, temperature and mass and mole fractions as well as their thermodynamic and Jacobian partial derivatives for five-species neutral equilibrium air. Applicable for arbitrary forms of equilibrium constants and especially designed for explicit and implicit CFD algorithms, the procedure algebraically reduces to two equations the six-equation thermodynamic system comprising the equations for internal energy, law of mass action and conservation of species mass and ratio of oxygen and nitrogen nuclei. This exact algebraic reduction explicitly expresses four mass fractions in terms of nitric oxide mass fraction and temperature, which are then determined through a rapidly converging numerical solution of the internal energy and nitric oxide mass action equations. The procedure then exactly determines the partial derivatives of pressure, temperature and mass fractions analytically. The mathematical formulation also introduces a convenient system non-dimensionalization that makes the procedure uniformly applicable to flows ranging from shock tube flows with zero initial velocity to aerothermodynamic flows with supersonic/hypersonic freestream Mach numbers. Over a wide range of density and internal energy the predicted distributions of mole fractions for the model five species agree with independent published results, while pressure and temperature as well as their partial derivatives remain continuous, smooth and physically meaningful. © 1997 John Wiley & Sons, Ltd.

Int. J. Numer. Meth. Fluids, **25**: 879–906 (1997)

No. of Figures: 7. No. of Tables: 1. No. of References: 11.

KEY WORDS: CFD; thermodynamic properties; equilibrium air

1. INTRODUCTION

For specified initial and boundary conditions for the Euler on Navier–Stokes conservation law system, the chemical dissociations within reacting air absorb energy and thus lead to lower static temperatures, higher static densities and different shock wave positions in comparison with perfect-air predictions. These effects must therefore be modelled accurately for a reliable CFD simulation of aerothermodynamic and high-temperature flows.

Either curve fits or solutions of the chemical equilibrium thermodynamics equations can be used to model the thermodynamic properties of reacting equilibrium air. Tannehill and Muge¹ have used their curve fits for time-dependent CFD calculations. Liou *et al.*² used Gordon and McBride's

*Correspondence to: J. Iannelli, Department of Mechanical & Aerospace Engineering and Engineering Science, The University of Tennessee, 315 Perkins Hall, Knoxville, TN 37996-2030, U.S.A.

procedure to generate equilibrium air thermodynamic properties that were then curve fitted to simulate numerically high-temperature shock tube flows. As another representative example, Prabhu *et al.*³ and Yee *et al.*⁴ use the Srinivasan curve fits for their numerical predictions of inviscid and viscous hypersonic flows. If a set of curve fits in turn depends on exponential correlations for the equilibrium constants, then when improved correlations become available, the curve fits will have to be revised. Furthermore, while many curve fits supply reliable values for pressure, temperature and other thermodynamic variables, the accuracy of the thermodynamic derivatives of these variables may be insufficient in some curve fits. For several CFD simulations of hypersonic flows, for instance, Yee *et al.*⁴ report a degradation in solution accuracy and stability as triggered by discontinuities in the curve-fitted thermodynamic derivatives.

As an alternative to curve-fitting methods, Park,⁵ Park and Yoon⁶ and Desideri *et al.*⁷ use solutions of classical chemical non-equilibrium and equilibrium thermodynamic systems in their CFD methods and report accurate solutions for several hypersonic blunt body flows. With these systems the partial derivatives of pressure and temperature can then be analytically determined by differentiating the thermodynamic equations. The results in these references, therefore, bear out the feasibility of coupling at each grid point the solution of a chemical equilibrium thermodynamic system with Euler and Navier–Stokes CFD algorithms.

This paper presents a computationally efficient solution procedure of an exact thermodynamic model for five-species, electrically neutral and chemically reacting air. The model involves an explicit pressure equation of state coupled to a non-linear system of six chemical equilibrium thermodynamic equations for five mass fractions and temperature. The resulting equations then revert to the familiar perfect gas expressions in the appropriate temperature and pressure ranges. The developed solution procedure remains valid for arbitrary forms of the equilibrium constants and, without introducing spurious solutions, succeeds in algebraically reducing this six-equation system to a two-equation system for nitric oxide mass fraction and temperature, which are then numerically determined through a rapidly converging Newton method solution. The remaining mass fractions and pressure are then explicitly calculated using this solution, while the thermodynamic and Jacobian derivatives of pressure and temperature are exactly determined through an analytical differentiation of the chemical equilibrium equations in the model.

Classical equilibrium thermodynamics for homogeneous fluids^{8,9} shows that pressure and temperature depend on only two other thermodynamic variables. For CFD applications the selected two thermodynamic variables are density and mass-specific internal energy, since these variables are directly available from the continuity and volume-specific total energy equations in the Euler and Navier–Stokes conservation law systems. In the equilibrium thermodynamic system, therefore, density and mass-specific internal energy become assigned parameters at each grid point.

The neutral air in the procedure encompasses perfect air and consists of a mixture of five non-ionized species: nitric oxide, NO, and molecular as well as atomic oxygen, O₂ and O, and nitrogen, N₂ and N. The choice of neutral air is justified by the independent Reference 10, which confirm that only negligible traces of electrons and hence ionic species exist within equilibrium air for temperatures below 8000 K. Each species independently behaves as a perfect gas for which the familiar perfect gas law applies. The mixture pressure equation of state is then obtained through Dalton's law as a sum of species partial pressures, which results in density and temperature multiplying a linear combination of mass fractions and molecular masses. The mixture mass-specific internal energy results from the sum of formation energy, translational and rotational kinetic energies and potential vibrational energy, all at the single equilibrium static temperature. The vibrational potential energy term in this equation relies upon the rigid rotor harmonic oscillator model,^{8,9} which implies the perfect gas equation of state for each species, which in turn is consistent with Dalton's law. Two additional equations correspond to the conservation of species mass and the mole ratio of oxygen and nitrogen nuclei.

The law of mass action provides the completing three equations, which express the equilibrium of any three linearly independent chemical reactions for the five species in equilibrium air.

For increased versatility the equilibrium thermodynamic equations are made non-dimensional by way of a convenient single reference state that makes the procedure uniformly applicable to flows ranging from shock tube flows with zero initial velocity to aerothermodynamic flows with supersonic/hypersonic freestream Mach numbers. Over a wide range of density and internal energy, corresponding to a temperature range of 8000 K and pressure range corresponding to an increase in altitude of over 30,000 m (100,000 ft) above sea level, the procedure converges in two or three iterations and generates distributions of mole fractions for the model five species that agree with independent published results, while pressure and temperature as well as their partial derivatives remain continuous, smooth and physically meaningful.

The remainder of this paper is organized in nine sections and five appendices. Section 2 presents the governing Euler and Navier–Stokes conservation law systems, along with a reference thermochemical equilibrium pressure equation of state and temperature equation, while Section 3 summarizes results for a perfect gas to simplify discussion of results in Section 9 and introduce principles, variables and constants needed for the more general chemical equilibrium model. Section 4 is devoted to the development of the equilibrium air seven-equation thermodynamic system. The reference variables and corresponding non-dimensional system are determined in Section 5, while the algebraic reduction and numerical solution are detailed in Sections 6 and 7. The analytical determination of the partial derivatives of pressure and temperature is then presented in Section 8, while Section 9 documents the computational results. Concluding remarks are made in Section 10. Finally, Appendices I–V detail all the thermodynamic data and Jacobian partial derivatives for immediate reproduction of the procedure and results.

2. NAVIER–STOKES CONSERVATION LAW SYSTEM, PRESSURE EQUATION OF STATE AND TEMPERATURE EQUATION

For arbitrary equilibrium fluids and with implied summation on repeated indices the multi-dimensional time-dependent governing Navier–Stokes equations in Cartesian conservation law system form are written as

$$\frac{\partial q}{\partial t} + \frac{\partial f_j(q)}{\partial x_j} = \frac{\partial f_j^v}{\partial x_j}. \tag{1}$$

The Euler equations can then be obtained from (1) by setting the right-hand side to zero identically. In (1), $1 \leq j \leq n$, where n denotes the number of spatial dimensions, $1 \leq n \leq 3$, while $\mathbf{x} \equiv (x_1, x_2, x_3) \in \Omega \subset \mathbb{R}^n$ and $t \in [t_0, \infty) \subset \mathbb{R}$ where \mathbb{R} denotes the field of real numbers and Ω indicates the solution domain.

The state variable q and the inviscid and viscous flux components f_j and f_j^v are defined as

$$q \equiv \begin{Bmatrix} \rho \\ m_1 \\ m_2 \\ m_3 \\ E \end{Bmatrix}, \quad f_j \equiv \begin{Bmatrix} m_j \\ \frac{m_j}{\rho} m_1 + p\delta_j^1 \\ \frac{m_j}{\rho} m_2 + p\delta_j^2 \\ \frac{m_j}{\rho} m_3 + p\delta_j^3 \\ \frac{m_j}{\rho} (E + p) \end{Bmatrix}, \quad f_j^v \equiv \begin{Bmatrix} 0 \\ \tau_{1j} \\ \tau_{2j} \\ \tau_{3j} \\ \sum_{i=1}^3 \frac{m_i}{\rho} \sigma_{ij} - q_j^{\mathcal{F}} \end{Bmatrix}. \tag{2}$$

In q and f_j the dependent variable ρ denotes the static density, E indicates the volume-specific total energy and $m_j = \rho u_j$ corresponds to the j th component of the volume-specific linear momentum \mathbf{m} , with u_j the corresponding component of the Eulerian velocity. The inviscid flux component f_j then depends on q as well as on the static pressure p , with δ_j^i , $1 \leq i \leq n$, defining the Kronecker delta, while the viscous flux component f_j^v depends on u_j as well as on the deviatoric stress tensor $[\tau_{ij}]$ and the Fourier heat flux component $q_j^{\mathcal{F}} = -k(T)\partial T/\partial x_j$, in terms of static temperature T , with $k(T)$ indicating the thermal conductivity.

For mathematical closure, therefore, the Euler and Navier–Stokes equations require an equation of state (EOS) relating the pressure p to the dependent variable q . The Navier–Stokes system must be further augmented with a constitutive relation for $[\tau_{ij}]$, an expression for $k(T)$ and a temperature equation (TE), independent of the EOS, relating T to q . Implicit Euler and Navier–Stokes CFD algorithms additionally require the Jacobian partial derivatives of p with respect to q and an implicit Navier–Stokes CFD algorithm also requires the Jacobian partial derivatives of T with respect to q .

Functionally cast, the EOS and TE are

$$p = p(q), \quad T = T(q). \tag{3}$$

For a homogeneous fluid in thermal and chemical equilibrium, thermodynamics stipulates p and T as each dependent upon two other thermodynamic variables according to

$$p = p(\rho, \varepsilon), \quad T = T(\rho, \varepsilon), \tag{4}$$

where ε denotes the mass-specific internal energy. For a given q this energy can be obtained from E , which is by definition the sum of volume-specific internal and kinetic energies. As a result,

$$E = \rho\varepsilon + \frac{1}{2\rho} \sum_{i=1}^n m_i m_i \Rightarrow \rho\varepsilon = E - \frac{1}{2\rho} \sum_{i=1}^n m_i m_i. \tag{5}$$

The functions that respectively relate the pressure p and temperature T to q are thus

$$p = p(\rho, \varepsilon(q)) = p(\rho, \varepsilon(\rho, \mathbf{m}, E)), \quad T = T(\rho, \varepsilon(q)) = T(\rho, \varepsilon(\rho, \mathbf{m}, E)). \tag{6}$$

Given q , therefore, p and T as well as their important partial derivatives with respect to q are obtained from (6) and the thermodynamic partial derivatives of (6) with respect to ρ and ε . The following sections present and solve the equations that lead to (6) for a neutral mixture of five species.

3. PERFECT GAS PRESSURE AND TEMPERATURE EQUATIONS

This section uses the well-known perfect gas EOS and TE to introduce the principles, variables and constants needed for the EOS and TE of an equilibrium multispecies reacting gas and to simplify the discussion of results in Section 9. From the works of Boyle, Mariotte, Charles and Gay-Lussac and the experiment of Joule respectively the EOS and TE for a perfect gas are

$$p = R\rho T, \quad \rho\varepsilon = \rho c_v T, \tag{7}$$

where R and c_v respectively denote the specific (not universal) gas constant and constant-volume specific heat. For a perfect gas, R and c_v are constant and related by Mayer’s equality $c_p - c_v = R$, where c_p indicates the constant-pressure specific heat. Through the ratio $\gamma = c_p/c_v$, Mayer’s equality then becomes $\gamma - 1 = R/c_v$. From this equality and (5) the elimination of T from (7) leads to the perfect gas EOS and TE forms

$$p = (\gamma - 1)\rho\varepsilon = (\gamma - 1)\left(E - \frac{1}{2\rho} \sum_{i=1}^n m_i m_i\right), \quad T = \frac{p}{\mathcal{R}\rho}, \tag{8}$$

two well-known expressions in CFD.

Perfect air is a mixture of two diatomic thermally and calorifically perfect gases: oxygen, O_2 , and nitrogen, N_2 , with molecular masses M_{O_2} and M_{N_2} . In terms of the universal gas constant \mathcal{R} (see Appendix I) the EOS for this perfect air is

$$p = \rho T \frac{\mathcal{R}}{M_{\text{air}}}, \quad (9)$$

where M_{air} denotes the molecular mass of air. This molecular mass is determined in terms of the molecular masses of O_2 and N_2 by way of Dalton's pressure law. This law stipulates that the overall mixture pressure results from the sum of partial pressure of the component gases and is thus expressed as

$$p = p_{O_2} + p_{N_2} = \rho_{O_2} T \frac{\mathcal{R}}{M_{O_2}} + \rho_{N_2} T \frac{\mathcal{R}}{M_{N_2}} = \rho \mathcal{R} T \left(\frac{Y_{O_2}}{M_{O_2}} + \frac{Y_{N_2}}{M_{N_2}} \right), \quad (10)$$

where ρ_{O_2} and ρ_{N_2} denote the partial densities of O_2 and N_2 respectively and $Y_{O_2} \equiv \rho_{O_2}/\rho$ and $Y_{N_2} \equiv \rho_{N_2}/\rho$ indicate the corresponding mass fractions. Since the right-hand sides (RHSs) of the EOS in (9) and (10) are equal to one another, the associated expression for M_{air} becomes

$$M_{\text{air}} = \left(\frac{Y_{O_2}}{M_{O_2}} + \frac{Y_{N_2}}{M_{N_2}} \right)^{-1}. \quad (11)$$

Similar to Dalton's law, the rule for determining the mixture TE in terms of the volume-specific internal energy $\rho\varepsilon$ involves the sum of volume-specific internal energies of the component species according to

$$\rho\varepsilon = \rho_{O_2} \varepsilon_{O_2} + \rho_{N_2} \varepsilon_{N_2} = \rho_{O_2} c_{v_{O_2}} T + \rho_{N_2} c_{v_{N_2}} T = \rho T (Y_{O_2} c_{v_{O_2}} + Y_{N_2} c_{v_{N_2}}). \quad (12)$$

Since the RHSs of the TEs in (7) and (12) equal one another, the expression for the mixture constant-volume specific heat becomes

$$c_{v_{\text{air}}} = Y_{O_2} c_{v_{O_2}} + Y_{N_2} c_{v_{N_2}}, \quad (13)$$

which is analogous to (11).

Expressions (9)–(13) thus show that the mixture pressure and temperature as well as the molecular mass and specific heat are directly determined for a given mixture density ρ and mass-specific internal energy ε when the mass fractions are known. In particular, a formulation in terms of mass fractions is convenient because the corresponding expressions for pressure and internal energy are linear with respect to the mass fractions, unlike a formulation in terms of mole fractions. The mass fractions can then be obtained either from additional chemical equilibrium equations or from chemical data for the corresponding mole fractions.

The mole fraction X of a species in a mixture is the ratio of species moles and total number of mixture moles. It turns out that for any chemical species that behaves as a perfect gas, X can also be named a 'pressure fraction', with an expression similar to that of the mass fraction, because from (9) and (10) the ratio of partial pressure and mixture pressure equals X . For O_2 in perfect or equilibrium reacting air, for instance, the corresponding mole fraction is expressed as $X_{O_2} = \mathcal{N}_{O_2}/\mathcal{N}$, where \mathcal{N}_{O_2} and \mathcal{N} respectively denote the numbers of moles of O_2 and air. Considering that $\rho_{O_2} = \mathcal{N}_{O_2} M_{O_2} / \mathcal{V}$,

where \mathcal{V} denotes the volume occupied by the mixture, the identity of mole and pressure fractions is then obtained as

$$\frac{p_{\text{O}_2}}{p} = \frac{\rho_{\text{O}_2}/M_{\text{O}_2}}{\rho/M} = \frac{(\mathcal{N}_{\text{O}_2}M_{\text{O}_2}/\mathcal{V})/M_{\text{O}_2}}{(\mathcal{N}M/\mathcal{V})/M} = \frac{\mathcal{N}_{\text{O}_2}}{\mathcal{N}} = X_{\text{O}_2}, \quad \frac{Y_{\text{O}_2}M_{\text{O}_2}}{M} = X_{\text{O}_2}, \quad (14)$$

where M denotes the molecular mass of reacting or non-reacting air.

The mole fractions then lead to the corresponding mass fractions as follows. From (14) and the definitions of air molecular mass, mass fraction and mole fraction the relations between the mass and mole fractions for the perfect air species are

$$X_{\text{O}_2} = \frac{Y_{\text{O}_2}/M_{\text{O}_2}}{Y_{\text{O}_2}/M_{\text{O}_2} + Y_{\text{N}_2}/M_{\text{N}_2}}, \quad X_{\text{N}_2} = \frac{Y_{\text{N}_2}/M_{\text{N}_2}}{Y_{\text{O}_2}/M_{\text{O}_2} + Y_{\text{N}_2}/M_{\text{N}_2}}. \quad (15)$$

For the well-known perfect air values $X_{\text{O}_2} = 0.21$ and $X_{\text{N}_2} = 0.79$ the corresponding mass fractions from (15) and associated perfect air molecular mass M_{air} , gas constant R and constant-volume specific heat $c_{v,\text{air}}$ are

$$Y_{\text{O}_2} = 0.232917001 \dots, \quad Y_{\text{N}_2} = 0.767008299 \dots, \quad (16)$$

$$M_{\text{air}} = (X_{\text{O}_2}M_{\text{O}_2} + X_{\text{N}_2}M_{\text{N}_2})/(Y_{\text{O}_2} + Y_{\text{N}_2}) = 28.85039719 \dots \text{ kg kg-mol}^{-1}, \quad (17)$$

$$R = 288.176275191 \dots \text{ J kg}^{-1} \text{ K}^{-1}, \quad c_{v,\text{air}} = 115.270510076 \dots \text{ J kg}^{-1} \text{ K}^{-1}. \quad (18)$$

For reacting air the mass fractions are no longer independent of temperature and can be determined by way of an equilibrium thermodynamic system as detailed in the following sections.

4. REACTING AIR EQUATIONS OF STATE

The equations in this section will represent equilibrium, electrically neutral and chemically reacting air. This type of air encompasses perfect air and consists of a mixture of five non-ionized species: nitric oxide, NO, and molecular as well as atomic oxygen, O₂ and O, and nitrogen, N₂ and N.

In the following, subscript i , $1 \leq i \leq 5$, indicates the five ordered species O, N, NO, O₂ and N₂, each with its own molecular mass M_i (see Appendix I) as well as partial density ρ_i and corresponding mass fraction $Y_i \equiv \rho_i/\rho$, with ρ the mixture density. Each species i independently behaves as a perfect gas with individual EOS

$$p_i = \mathcal{R}T \frac{\rho_i}{M_i}. \quad (19)$$

For a mixture of perfect species, therefore, Dalton's law leads to the mixture pressure equation of state as

$$p = \sum_{i=1}^5 p_i = \mathcal{R}\rho T \sum_{i=1}^5 \frac{Y_i}{M_i}, \quad (20)$$

which generalizes (9).

The mixture mass-specific internal energy ε results from the sum of formation energy, translational and rotational kinetic energies and potential vibrational energy, all at the equilibrium static temperature T , in the form

$$\varepsilon = T \sum_{i=1}^5 c_{v_i} Y_i + \sum_{i=3}^5 \frac{Y_i \mathcal{R} \theta_i^v / M_i}{\exp(\theta_i^v / T) - 1} + \sum_{i=1}^3 Y_i h_i^0, \quad (21)$$

which generalizes the TE in (7). The second term on the RHS of (21) relies upon the rigid rotor harmonic oscillator model,^{8,9} which implies the perfect gas equation of state for each species, which in turn is consistent with Dalton's pressure-mixing rule. Therefore the contributions from the ground electronic state are properly modelled for N₂, O₂ and NO. Certainly, these molecules are known to behave like anharmonic oscillators, and considering that the contribution to vibrational heat capacity from the first anharmonicity term alone is about (4, 7, 5)% at 5000 K and about (7, 14, 10)% at 10,000 K, equation (21) is accurate for $T < 10,000$ K. In (21), c_{v_i} denotes the translational/rotational mode contributions to the i th-species constant-volume specific heat, while θ_i^v and h_i^0 respectively are the vibrational temperature and formation enthalpy at 0 K; specific numerical data for these quantities appear in Appendix I.

Considering that both ρ and ε are available at each grid point from the conservation law system (1), (5), equations (20) and (21) will directly allow the determination of static temperature T and pressure p for the given thermodynamic state (ρ , ε). Fundamental to this determination are the five variable mass fractions Y_i , $1 \leq i \leq 5$, for which five additional equations are needed.

One equation corresponds to the conservation of species mass⁸ in the form $\sum_{i=1}^5 \rho_i = \rho$, which results in the mass fraction conservation equation

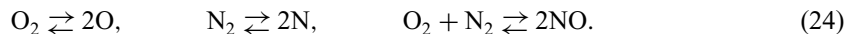
$$\sum_{i=1}^5 Y_i = 1. \quad (22)$$

Another equation corresponds to the conservation of the mole proportion 21/79 between oxygen and nitrogen nuclei. In terms of mole fractions the conservation of this proportion is expressed as $79(X_1 + X_3 + 2X_4) = 21(X_2 + X_3 + 2X_5)$, which, by virtue of expressions similar to (14) for the generic species i , corresponds to the following equation in terms of mass fractions:

$$\frac{1}{21} \left(\frac{Y_1}{M_1} + \frac{Y_3}{M_3} + 2 \frac{Y_4}{M_4} \right) = \frac{1}{79} \left(\frac{Y_2}{M_2} + \frac{Y_3}{M_3} + 2 \frac{Y_5}{M_5} \right). \quad (23)$$

The law of mass action provides three further equations, which express the equilibrium of any three linearly independent chemical reactions for the five species in equilibrium air. That the number n_{MA} of linearly independent mass action equations is three for the subject five-species air follows from the simple rule $n_{\text{MA}} = (\text{number of species}) - (\text{number of elements}) = 3$.⁸

The following chemical reactions, two dissociations and one recombination, lead to computationally convenient mass action equations:



In terms of partial pressures, the mass action equations for reactions (24) are

$$\frac{p_1^2}{p_4} = k_1(T), \quad \frac{p_2^2}{p_5} = k_2(T), \quad \frac{p_3^2}{p_4 p_5} = k_3(T), \quad (25)$$

and according to statistical thermodynamics,^{8,9} the partial-pressure equilibrium functions $k_i(T)$ only depend on the static temperature T and the stoichiometric coefficients in (24) become the exponents in (25). Replacing the partial pressure p_i using (19) yields the mass-fraction law of mass action as

$$\frac{Y_1^2}{Y_4} = \frac{M_1^2 k_1(T)}{M_4 \mathcal{R}T\rho} = \frac{M_1^2 K_1(T)}{M_4 \rho}, \quad (26)$$

$$\frac{Y_2^2}{Y_5} = \frac{M_2^2 k_2(T)}{M_5 \mathcal{R}T\rho} = \frac{M_2^2 K_2(T)}{M_5 \rho}, \quad (27)$$

$$\frac{Y_3^2}{Y_4 Y_5} = \frac{M_3^2}{M_4 M_5} K_3(T), \quad (28)$$

where $K_i(T)$, $1 \leq i \leq 3$, represent the mass fraction equilibrium functions, which are traditionally cast as exponential relations,^{5,6,9,10} as exemplified in Appendix II. According to the dimensions of terms in (26)–(28), the SI units of $K_1(T)$ and $K_2(T)$ are $\text{kg}\cdot\text{mol}^{-1} \text{kg m}^{-3}$, whereas $K_3(T)$ remains dimensionless. The following analytical developments will remain valid for any form of these equilibrium functions.

5. NON-DIMENSIONAL REACTING AIR EQUATIONS OF STATE

For increased versatility the system of equations (20)–(23), (26)–(28) is made non-dimensional by way of a convenient single reference state that makes this system uniformly applicable to flows ranging from flows with a specified fixed initial state with zero velocity, typical of shock tube flows, to flows with an identifiable freestream state, typical of supersonic/hypersonic aerothermodynamic flows.

For an available freestream state with representative constant pressure p_∞ , temperature T_∞ , density ρ_∞ and Mach number \mathcal{M}_∞ the reference molecular mass, density, mass-specific energy (speed squared), pressure and temperature are expressed as

$$\begin{aligned} M_a &= \frac{\mathcal{R}\rho_\infty T_\infty}{p_\infty}, & \rho_r &= \frac{p_\infty}{(\mathcal{R}/M_a)T_\infty}, \\ U_r^2 &= \gamma \mathcal{M}_\infty^2 (\mathcal{R}/M_a) T_\infty, & p_r &= \rho_r U_r^2 = \gamma \mathcal{M}_\infty^2 p_\infty, \\ T_r &= \frac{p_r}{\rho_r (\mathcal{R}/M_a)} = \frac{U_r^2}{\mathcal{R}/M_a} = \gamma \mathcal{M}_\infty^2 T_\infty, \end{aligned} \quad (29)$$

where $\gamma = 1.4$, the constant ratio of perfect air specific heats, is introduced in (29) so that U_r becomes the flow speed when the corresponding freestream gas is perfect air. If ρ_∞ , p_∞ and T_∞ already satisfy the perfect gas law, then the reference molecular mass M_a corresponds to the air molecular mass; otherwise, it simply represents a scaling factor by which to divide the species molecular masses. Either way, $\rho_r = \rho_\infty$ with this particular choice. With definitions (29) the reference pressure, density and temperature then satisfy the perfect gas law and for high Mach numbers they constitute sizable constants that conveniently scale down the large pressure, density and temperature across the stagnation-streamline normal section of supersonic and hypersonic aerodynamic-flow bow shocks.

For a typical shock-tube initial state with representative constant pressure p_∞ , temperature T_∞ and density ρ_∞ the reference variables are

$$\begin{aligned} M_a &= \frac{\mathcal{R}\rho_\infty T_\infty}{p_\infty}, & \rho_r &= \frac{p_\infty}{(\mathcal{R}/M_a)T_\infty}, \\ U_r^2 &= p_r/\rho_r = (\mathcal{R}/M_a)T_\infty = \gamma \mathcal{M}_r^2 (\mathcal{R}/M_a)T_\infty, & \gamma \mathcal{M}_r^2 &= 1, \\ p_r &= p_\infty = \gamma \mathcal{M}_r^2 p_\infty, & T_r &= T_\infty = \gamma \mathcal{M}_r^2 T_\infty \end{aligned} \tag{30}$$

and, as before, $\rho_r = \rho_\infty$ while p_∞ , ρ_∞ and T_∞ satisfy the perfect gas law. Importantly, for $\gamma \mathcal{M}_r^2 = 1$, hence $\mathcal{M}_r^2 = 1/\gamma$, this reference state formally coincides with (29). Therefore setting \mathcal{M}_r equal to either \mathcal{M}_∞ or $1/\gamma$, depending on the flow class, leads to a unique set of non-dimensional equations of state for both reference sets (29) and (30).

Using the reference states (29) or (30), the non-dimensional density, mass-specific internal energy, pressure and temperature are then expressed as

$$\tilde{\rho} = \frac{\rho}{\rho_r}, \quad \tilde{\varepsilon} = \frac{\varepsilon}{U_r^2} = \frac{\varepsilon}{\gamma \mathcal{M}_r^2 (\mathcal{R}/M_a)T_\infty}, \quad \tilde{p} = \frac{p}{p_r}, \quad \tilde{T} = \frac{T}{T_r} = \frac{T}{\gamma \mathcal{M}_r^2 T_\infty}. \tag{31}$$

The corresponding non-dimensional pressure equation is

$$\tilde{p} = \frac{\mathcal{R}\rho T \rho_r T_r}{\rho_r T_r p_r} \sum_{i=1}^5 \frac{y_i}{M_i} = \frac{\mathcal{R}\rho T}{(\mathcal{R}/M_a)\rho_r T_r} \sum_{i=1}^5 \frac{Y_i}{M_i} = \tilde{\rho} \tilde{T} \sum_{i=1}^5 \frac{Y_i}{M_i/M_a} = \tilde{\rho} \tilde{T} \sum_{i=1}^5 \frac{Y_i}{\tilde{M}_i}. \tag{32}$$

Hence the universal gas constant \mathcal{R} no longer appears in this non-dimensional equation of state. The non-dimensional energy equation is

$$\tilde{\varepsilon} = \frac{T}{\gamma \mathcal{M}_r^2 (\mathcal{R}/M_a)T_\infty} \sum_{i=1}^5 c_{v_i} Y_i + \sum_{i=3}^5 \frac{Y_i \mathcal{R} \theta_i^v / M_i}{[\gamma \mathcal{M}_r^2 (\mathcal{R}/M_a)T_\infty][\exp(\theta_i^v/T) - 1]} + \sum_{i=1}^3 Y_i \frac{h_i^0}{\gamma \mathcal{M}_r^2 (\mathcal{R}/M_a)T_\infty}, \tag{33}$$

which as simplified as

$$\tilde{\varepsilon} = \tilde{T} \sum_{i=1}^5 \tilde{c}_{v_i} Y_i + \sum_{i=3}^5 \frac{Y_i \tilde{\theta}_i^v / \tilde{M}_i}{\exp(\tilde{\theta}_i^v / \tilde{T}) - 1} + \sum_{i=1}^3 Y_i \tilde{h}_i^0 \tag{34}$$

and the universal gas constant \mathcal{R} no longer multiplies any term in (34). Furthermore, as indicated in Appendix I, the magnitudes of the non-dimensional specific heat \tilde{c}_{v_i} , characteristic vibrational temperature $\tilde{\theta}_i^v$ and formation enthalpy \tilde{h}_i^0 decrease with respect to their dimensional values.

Since the mass fractions Y_i are already dimensionless variables, the non-dimensional species conservation equations are

$$\sum_{i=1}^5 Y_i = 1, \quad \frac{1}{21} \left(\frac{Y_1}{\tilde{M}_1} + \frac{Y_3}{\tilde{M}_3} + 2 \frac{Y_4}{\tilde{M}_4} \right) = \frac{1}{79} \left(\frac{Y_2}{\tilde{M}_2} + \frac{Y_3}{\tilde{M}_3} + 2 \frac{Y_5}{\tilde{M}_5} \right). \tag{35}$$

The non-dimensional mass action equations are then

$$\frac{Y_1^2}{Y_4} = \frac{\tilde{M}_1^2}{\tilde{M}_4} \frac{K_1(\tilde{T})}{\tilde{\rho}(\rho_r/M_a)} = \frac{\tilde{M}_1^2}{\tilde{M}_4} \frac{\tilde{K}_1(\tilde{T})}{\tilde{\rho}}, \tag{36}$$

$$\frac{Y_2^2}{Y_5} = \frac{\tilde{M}_2^2}{\tilde{M}_5} \frac{K_2(\tilde{T})}{\tilde{\rho}(\rho_r/M_a)} = \frac{\tilde{M}_2^2}{\tilde{M}_5} \frac{\tilde{K}_2(\tilde{T})}{\tilde{\rho}}, \tag{37}$$

$$\frac{Y_3^2}{Y_4 Y_5} = \frac{\tilde{M}_3^2}{\tilde{M}_4 \tilde{M}_5} \tilde{K}_3(\tilde{T}), \tag{38}$$

where $\tilde{K}_j, 1 \leq j \leq 3$, denote the non-dimensional equilibrium functions, as exemplified in Appendix II.

6. ALGEBRAIC REDUCTION

Grouped below for convenience, the non-dimensional equations of state are

$$\tilde{p} = \tilde{p}\tilde{T} \sum_{i=1}^5 \frac{Y_i}{\tilde{M}_i}, \tag{39}$$

$$\tilde{\varepsilon} = \tilde{T} \sum_{i=1}^5 \tilde{c}_{v,i} Y_i + \sum_{i=3}^5 \frac{Y_i \tilde{\theta}_i^v / \tilde{M}_i}{\exp(\tilde{\theta}_i^v / \tilde{T}) - 1} + \sum_{i=1}^3 Y_i \tilde{h}_i^0, \tag{40}$$

$$\sum_{i=1}^5 Y_i = 1, \tag{41}$$

$$\frac{1}{21} \left(\frac{Y_1}{\tilde{M}_1} + \frac{Y_3}{\tilde{M}_3} + 2 \frac{Y_4}{\tilde{M}_4} \right) = \frac{1}{79} \left(\frac{Y_2}{\tilde{M}_2} + \frac{Y_3}{\tilde{M}_3} + 2 \frac{Y_5}{\tilde{M}_5} \right), \tag{42}$$

$$\frac{Y_1^2}{Y_4} = \frac{\tilde{M}_1^2}{\tilde{M}_4} \frac{\tilde{K}_1(\tilde{T})}{\tilde{\rho}} = \tilde{M}_1^2 C_1, \tag{43}$$

$$\frac{Y_2^2}{Y_5} = \frac{\tilde{M}_2^2}{\tilde{M}_5} \frac{\tilde{K}_2(\tilde{T})}{\tilde{\rho}} = \tilde{M}_2^2 C_2, \tag{44}$$

$$\frac{Y_3^2}{Y_4 Y_5} = \frac{\tilde{M}_3^2}{\tilde{M}_4 \tilde{M}_5} \tilde{K}_3(\tilde{T}) = \tilde{M}_3^2 C_3, \tag{45}$$

where $C_i \equiv \tilde{K}_i(\tilde{T}) / (\tilde{\rho} \tilde{M}_{i+3}), i = 1, 2$, and $C_3 \equiv \tilde{K}_3(\tilde{T}) / (\tilde{M}_4 \tilde{M}_5)$. In the sequel the tilde is dropped from the system variables for simplicity.

The five mass fractions $Y_i, 1 \leq i \leq 5$, and static temperature T can then be theoretically obtained by solving the non-linear system of the last six equations given above and practically determined through a numerical iterative procedure, which for CFD applications would become a daunting proposition if such a 6×6 system required even a few iterations at each of hundreds of thousands of grid points. In the following developments, however, the four variable mass fractions $Y_i, i = 1, 2, 3, 4, 5$, of the six variables in this 6×6 system are explicitly expressed algebraically in terms of only two variables, temperature T and nitric oxide mass fraction Y_3 , and the complete solution of system (39)–(45) is obtained from the solution for these two variables of a far less

daunting 2×2 system. The selection of the specific relations leading to this system was predicated on the elimination of the potential spurious solutions that can be introduced in the algebraic manipulation of non-linear equations involving raising of powers. This criterion ensured that the resulting equations only possess a physically meaningful solution.

The two mass fractions Y_1 and Y_2 in the two linear equations (41) and (42) can be explicitly solved for in terms of Y_3 , Y_4 and Y_5 . The expression for Y_1 results by summing (42) to the product of (41) and $1/(79M_2)$, while that for Y_2 results by summing (42) to the products of (41) and $-1/(21M_1)$. This sequence of operations yields the expressions

$$Y_1 = \frac{0.21M_4}{M_{\text{air}}} - \frac{M_1}{M_3} Y_3 - Y_4, \quad (46)$$

$$Y_2 = \frac{0.79M_5}{M_{\text{air}}} - \frac{M_2}{M_3} Y_3 - Y_5, \quad (47)$$

which identically revert to (15) for vanishing Y_1 , Y_2 and Y_3 , where M_{air} is the constant perfect air molecular mass (17). For conciseness these two expressions are then cast as

$$Y_1 = \alpha_{10} - \alpha_{13} Y_3 - Y_4, \quad (48)$$

$$Y_2 = \alpha_{20} - \alpha_{23} Y_3 - Y_5, \quad (49)$$

where the constants α_{10} , α_{13} , α_{20} and α_{23} follow from inspection of (46) and (47).

The additional explicit relations for Y_4 and Y_5 result from inserting (48) and (49) into (43) and (44) respectively. This operation yields the quadratic equations

$$Y_4^2 - 2\left(\alpha_{10} - \alpha_{13} Y_3 + \frac{M_1^2 C_1}{2}\right) Y_4 + (\alpha_{10} - \alpha_{13} Y_3)^2 = 0, \quad (50)$$

$$Y_5^2 - 2\left(\alpha_{20} - \alpha_{23} Y_3 + \frac{M_2^2 C_2}{2}\right) Y_5 + (\alpha_{20} - \alpha_{23} Y_3)^2 = 0, \quad (51)$$

which remains valid for any equilibrium function $K_i(T)$, $i = 1, 2, 3$, and intrinsically depend upon Y_3 . Of the two mathematical solutions for each of (50) and (51) the solution devoid of physical significance is discarded and the physically meaningful solutions are then established as

$$Y_4 = \alpha_{10} - \alpha_{13} Y_3 + \frac{M_1^2 C_1}{2} - \left[M_1^2 C_1 \left(\alpha_{10} - \alpha_{13} Y_3 + \frac{M_1^2 C_1}{4} \right) \right]^{1/2}, \quad (52)$$

$$Y_5 = \alpha_{20} - \alpha_{23} Y_3 + \frac{M_2^2 C_2}{2} - \left[M_2^2 C_2 \left(\alpha_{20} - \alpha_{23} Y_3 + \frac{M_2^2 C_2}{4} \right) \right]^{1/2}. \quad (53)$$

According to the algebraic sign of the coefficients in (52) and (53), Y_4 and Y_5 are positive if so are the expressions $\alpha_{10} - \alpha_{13} Y_3$, $i = 1, 2$, since C_1 and C_2 are intrinsically positive. Given the definition of the coefficients α_{10} , α_{13} , α_{20} and α_{23} in (48) and (49), this condition is always met, since Y_3 stays below one. Furthermore, for increasing temperature both Y_4 and Y_5 from (52) and (53) consistently approach zero, as physically correct, owing to the monotonic increase in C_1 and C_2 . Finally, at lower temperatures, C_1 , C_2 and Y_3 approach zero. Hence Y_4 and Y_5 from (52) and (53) converge to their respective perfect gas values, while from (46) and (47) both Y_1 and Y_2 vanish.

By virtue of (52) and (53), Y_4 and Y_5 are functionally expressed as

$$Y_4 = Y_4(Y_3(\rho, \varepsilon), T(\rho, \varepsilon), \rho), \quad Y_5 = Y_5(Y_3(\rho, \varepsilon), T(\rho, \varepsilon), \rho) \quad (54)$$

and the functional relations for Y_1 and Y_2 from (46) and (47) are then

$$Y_1 = Y_1(Y_3(\rho, \varepsilon), Y_4(Y_3(\rho, \varepsilon), T(\rho, \varepsilon), \rho)), \quad Y_2 = Y_2(Y_3(\rho, \varepsilon), Y_5(Y_3(\rho, \varepsilon), T(\rho, \varepsilon), \rho)), \quad (55)$$

which show that these four mass fractions explicitly depend upon ρ and ε as well as upon Y_3 and T . For the thermodynamic state (ρ, ε) , existing at each grid node from (5) and the continuity and energy conservation equations in (1), and associated Y_3 and T , therefore, both Y_4 and Y_5 are directly obtained from (52) and (53), which then allows determining both Y_1 and Y_2 from (48) and (49). The corresponding pressure is then determined using (39). A complete solution for the non-linear six-equation system (40)–(45) is thus obtained when both Y_3 and T are determined.

7. TWO-EQUATION SYSTEM FOR Y_3 AND T

The two equations that remain to be solved for system (40)–(45) are the nitric oxide mass action equation (45) and the mass-specific internal energy equation (40). The solution for T and Y_3 is thus determined by solving the two-equation system

$$f_1(Y_3, T) \equiv Y_3 - M_3(Y_4 Y_5 C_3)^{1/2} = 0, \quad (56)$$

$$f_2(Y_3, T) \equiv \varepsilon - T \sum_{i=1}^5 c_{v_i} Y_i - \sum_{i=3}^5 \frac{Y_i \theta_i^v / M_i}{\exp(\theta_i^v / T) - 1} - \sum_{i=1}^3 Y_i h_i^0 = 0, \quad (57)$$

with $Y_i, i = 1, 2, 3, 4, 5$, expressed via (48)–(51). For a positive thermodynamic state (ρ, ε) each term in (56) and (57), with the exception of ε , is a non-positive monotone function of temperature T and nitric oxide mass fraction Y_3 . Furthermore, the square root expression in (56) is also a non-positive monotone function of T . Therefore a solution of system (56), (57) with positive Y_3 and T exists and is unique. This solution is numerically determined by solving this system through Newton's method.

7.1. Numerical solution

In system (56), (57) the thermodynamic state (ρ, ε) is known at each grid point. For the auxiliary variable $Q \equiv \{Y_3, T\}^T$, therefore, this system is cast as

$$F(\rho, \varepsilon, Q) \equiv F(\rho, \varepsilon, Y_3, T) \equiv \begin{Bmatrix} f_1(\rho, \varepsilon, Y_3, T) \\ f_2(\rho, \varepsilon, Y_3, T) \end{Bmatrix} = 0. \quad (58)$$

The Newton algorithm to solve (58) is

$$Q^{s+1} = Q^s - \left[\left(\frac{\partial F}{\partial Q} \right)_{\rho, \varepsilon}^s \right]^{-1} \{F^s\}, \quad (59)$$

where superscript s denotes the iteration index. The initial estimate Q^0 at a grid node can coincide with the value of Q at an adjacent grid point where this system has already been solved. If no solution for Q is available at an adjacent node, as is typical when system (56), (57) is solved at the first grid node, then an initial estimate for Q^0 can correspond to low T and consequently $Y_3 \equiv 0$. These two selections are consistent with each other, because C_3, Y_1 and Y_2 approach zero at lower temperatures, which leads to a vanishing Y_3 as a solution of (56). Under the same low-temperature conditions, equations (56) and (58) then asymptotically converge to the corresponding perfect gas expressions. With symmetrized f_1 and f_2 with respect to the f -axis, i.e. $f_i(-Y_3, -T) = f_i(Y_3, T)$ and $f_2(-Y_3, -T) = f_2(Y_3, T)$, the absolute values of both Y_3^s and T^s at the end of each iteration will

equally lead to the solution of (56) and (57), as also indicated in Reference 11 for a hydrocarbon equilibrium thermodynamic system. Iteration (59) is cast in closed form, since the 2×2 Jacobian is analytically determined in the following section. Hence evaluating (59) is relatively inexpensive, leads to a quadratically convergent process and directly yields Y_3 and T .

7.2. Iteration partial derivatives

For a given flow state $q \equiv \{\rho, \mathbf{m}, E\}^T$ and hence for a fixed (ρ, ε) , system (56), (57) is functionally cast as

$$f_1(\rho, Y_3, Y_4(Y_3, T, \rho), Y_5(Y_3, T, \rho), T) = 0, \tag{60}$$

$$f_2(\varepsilon, T, Y_1(Y_3, Y_4(Y_3, T, \rho)), Y_2(Y_3, Y_5(Y_3, T, \rho)), Y_3, Y_4(Y_3, T, \rho), Y_5(Y_3, T, \rho)) = 0. \tag{61}$$

Therefore the partial derivatives in the Jacobian matrix in (59) are expressed as

$$\left[\begin{matrix} \frac{\partial F}{\partial Q} \end{matrix} \right]_q \equiv \left[\begin{matrix} \left(\frac{\partial f_1}{\partial Y_3} \right)_{q,T}, & \left(\frac{\partial f_1}{\partial T} \right)_{q,Y_3} \\ \left(\frac{\partial f_2}{\partial Y_3} \right)_{q,T}, & \left(\frac{\partial f_2}{\partial T} \right)_{q,Y_3} \end{matrix} \right], \tag{62}$$

where subscripts denote the variables held constant in the partial differentiation. The partial derivatives in (62) are thus determined by application of the chain rule to (56) and (57), which yields the unabridged forms

$$\left(\frac{\partial f_1}{\partial Y_3} \right)_{q,T} = \left(\frac{\partial f_1}{\partial Y_3} \right)_{q,Y_4,Y_5,T} + \left(\frac{\partial f_1}{\partial Y_4} \right)_{q,Y_3,Y_5,T} \left(\frac{\partial Y_4}{\partial Y_3} \right)_{q,T} + \left(\frac{\partial f_1}{\partial Y_5} \right)_{q,Y_3,Y_4,T} \left(\frac{\partial Y_5}{\partial Y_3} \right)_{q,T} \tag{63}$$

$$\left(\frac{\partial f_1}{\partial T} \right)_{q,Y_3} = \left(\frac{\partial f_1}{\partial T} \right)_{q,Y_4,Y_5,Y_3} + \left(\frac{\partial f_1}{\partial Y_4} \right)_{q,Y_3,Y_5,T} \left(\frac{\partial Y_4}{\partial T} \right)_{q,Y_3} + \left(\frac{\partial f_1}{\partial Y_5} \right)_{q,Y_3,Y_4,T} \left(\frac{\partial Y_5}{\partial T} \right)_{q,Y_3}, \tag{64}$$

$$\begin{aligned} \left(\frac{\partial f_2}{\partial Y_3} \right)_{q,T} &= \left(\frac{\partial f_2}{\partial Y_3} \right)_{q,Y_1,Y_2,Y_4,Y_5,T} + \left(\frac{\partial f_2}{\partial Y_1} \right)_{q,Y_2,Y_3,Y_4,Y_5,T} \left(\frac{\partial Y_1}{\partial Y_3} \right)_{q,T} + \left(\frac{\partial f_2}{\partial Y_2} \right)_{q,Y_1,Y_3,Y_4,Y_5,T} \left(\frac{\partial Y_2}{\partial Y_3} \right)_{q,T} \\ &+ \left(\frac{\partial f_2}{\partial Y_4} \right)_{q,Y_1,Y_2,Y_3,Y_5,T} \left(\frac{\partial Y_4}{\partial Y_3} \right)_{q,T} + \left(\frac{\partial f_2}{\partial Y_5} \right)_{q,Y_1,Y_2,Y_3,Y_4,T} \left(\frac{\partial Y_5}{\partial Y_3} \right)_{q,T} \end{aligned} \tag{65}$$

$$\begin{aligned} \left(\frac{\partial f_2}{\partial T} \right)_{q,Y_3} &= \left(\frac{\partial f_2}{\partial T} \right)_{q,Y_1,Y_2,Y_3,Y_4,Y_5} + \left(\frac{\partial f_2}{\partial Y_1} \right)_{q,Y_2,Y_3,Y_4,Y_5,T} \left(\frac{\partial Y_1}{\partial T} \right)_{q,Y_3} + \left(\frac{\partial f_2}{\partial Y_2} \right)_{q,Y_1,Y_3,Y_4,Y_5,T} \left(\frac{\partial Y_2}{\partial T} \right)_{q,Y_3} \\ &+ \left(\frac{\partial f_2}{\partial Y_4} \right)_{q,Y_1,Y_2,Y_3,Y_5,T} \left(\frac{\partial Y_4}{\partial T} \right)_{q,Y_3} + \left(\frac{\partial f_2}{\partial Y_5} \right)_{q,Y_1,Y_2,Y_3,Y_4,T} \left(\frac{\partial Y_5}{\partial T} \right)_{q,Y_3}. \end{aligned} \tag{66}$$

Despite their deceptive complexity, these expressions become peculiarly simple, as detailed in Appendix III. With these analytical partial derivatives the procedure for determining temperature and the five mass fractions is theoretically complete. Therefore a practical implementation utilizes expressions (52), (53) and (48), (49) to compute $Y_i, i \neq 3$, for a given state (ρ, ε) at each grid point and associated (Y_3, T) . All these variables are then employed to evaluate functions (56) and (57) and all the partial derivatives (63)–(66) for the Newton-algorithm determination of Y_3 and T . The computational results discussed in Section 9 indicate that this procedure rapidly converges in two or three iterations and directly yields temperature and the five mass fractions. Pressure is then explicitly computed using (39).

8. JACOBIAN PARTIAL DERIVATIVES OF PRESSURE AND TEMPERATURE

As is well known, the convergence of implicit Euler and Navier–Stokes CFD algorithms critically depends upon accurate and continuous Jacobians of pressure with respect to the state variable q .⁴ Implicit Navier–Stokes CFD algorithms also require accurate and continuous Jacobians of temperature with respect to q . This section shows that the developed procedure leads to exact and smooth pressure and temperature Jacobian partial derivatives on the basis of the partial derivatives of $F(\rho, \varepsilon, Q)$ in (58) and $Y_i, 1 \leq i \leq 5$, with respect to ρ and ε .

To begin with, an application of the chain rule to the EOS in (6), $p = p(\rho, \varepsilon(q))$, leads to the partial derivatives of pressure with respect to the flow variable $q \equiv \{\rho, \mathbf{m}, E\}^T$ as

$$\left(\frac{\partial p}{\partial \rho}\right)_{\mathbf{m}, E} = \left(\frac{\partial p}{\partial \rho}\right)_{\varepsilon} + \left(\frac{\partial p}{\partial \varepsilon}\right)_{\rho} \left(\frac{\partial \varepsilon}{\partial \rho}\right)_{\mathbf{m}, E} = \left(\frac{\partial p}{\partial \rho}\right)_{\varepsilon} + \left(\frac{\partial p}{\partial \varepsilon}\right)_{\rho} \frac{1}{\rho^2} \left(\frac{1}{\rho} \sum_{i=1}^n m_i m_i - E\right), \tag{67}$$

$$\left(\frac{\partial p}{\partial m_i}\right)_{\rho, m_j, E, i \neq j} = \left(\frac{\partial p}{\partial \varepsilon}\right)_{\rho} \left(\frac{\partial \varepsilon}{\partial m_i}\right)_{\rho, m_j, E, i \neq j} = \left(\frac{\partial p}{\partial \varepsilon}\right)_{\rho} \left(-\frac{m_i}{\rho^2}\right), \tag{68}$$

$$\left(\frac{\partial p}{\partial E}\right)_{\rho, \mathbf{m}} = \left(\frac{\partial p}{\partial \varepsilon}\right)_{\rho} \left(\frac{\partial \varepsilon}{\partial E}\right)_{\rho, \mathbf{m}} = \left(\frac{\partial p}{\partial \varepsilon}\right)_{\rho} \left(\frac{1}{\rho}\right). \tag{69}$$

The corresponding partial derivatives of T are directly obtained by replacing p with T in (67)–(69).

As noted in Sections 6 and 7, equations (48), (49), (52), (53) and (56), (57) asymptotically approach the perfect gas expressions. Therefore (67)–(69) will converge to the perfect gas partial derivatives at low temperatures. For the reacting flow case these Jacobian derivatives depend on the thermodynamic derivatives $(\partial p/\partial \rho)_{\varepsilon}$ and $(\partial p/\partial \varepsilon)_{\rho}$. Similarly, the Jacobian partial derivatives of T depend on the thermodynamic derivatives $(\partial T/\partial \rho)_{\varepsilon}$ and $(\partial T/\partial \varepsilon)_{\rho}$.

These thermodynamic derivatives of pressure are determined exactly by differentiating the EOS (39) in the form

$$\left(\frac{\partial p}{\partial \rho}\right)_{\varepsilon} = T \sum_{i=1}^5 \frac{Y_i}{M_i} + \rho \left(\frac{\partial T}{\partial \rho}\right)_{\varepsilon} \sum_{i=1}^5 \frac{Y_i}{M_i} + \rho T \sum_{i=1}^5 \frac{1}{M_i} \left(\frac{\partial Y_i}{\partial \rho}\right)_{\varepsilon}, \tag{70}$$

$$\left(\frac{\partial p}{\partial \varepsilon}\right)_{\rho} = \rho \left(\frac{\partial T}{\partial \varepsilon}\right)_{\rho} \sum_{i=1}^5 \frac{Y_i}{M_i} + \rho T \sum_{i=1}^5 \frac{1}{M_i} \left(\frac{\partial Y_i}{\partial \varepsilon}\right)_{\rho}, \tag{71}$$

which shows the dependence on the thermodynamic derivatives of both T and mass fractions $Y_i, 1 \leq i \leq 5$, with respect to ρ and ε . These thermodynamic derivatives are determined through system (58) as follows.

Considering that $Q = Q(\rho, \varepsilon)$, the differential of both sides of expression (58) yields

$$\left[\left(\frac{\partial F}{\partial Q}\right)_{\rho, \varepsilon} \left(\frac{\partial Q}{\partial \rho}\right)_{\varepsilon} + \left(\frac{\partial F}{\partial \rho}\right)_{Q, \varepsilon} \right] d\rho + \left[\left(\frac{\partial F}{\partial Q}\right)_{\rho, \varepsilon} \left(\frac{\partial Q}{\partial \varepsilon}\right)_{\rho} + \left(\frac{\partial F}{\partial \varepsilon}\right)_{Q, \rho} \right] d\varepsilon = 0. \tag{72}$$

This constitutes a linear combination on the linearly independent differentials $d\rho$ and $d\varepsilon$, holding true if and only if their coefficients independently vanish, which defines the two linear systems

$$\left(\frac{\partial Q}{\partial \rho}\right)_{\varepsilon} = - \left[\left(\frac{\partial F}{\partial Q}\right)_{\rho, \varepsilon} \right]^{-1} \left(\frac{\partial F}{\partial \rho}\right)_{Q, \varepsilon}, \quad \left(\frac{\partial Q}{\partial \varepsilon}\right)_{\rho} = - \left[\left(\frac{\partial F}{\partial Q}\right)_{\rho, \varepsilon} \right]^{-1} \left(\frac{\partial F}{\partial \varepsilon}\right)_{Q, \rho}. \tag{73}$$

The Jacobian in both of these expressions is invariant and coincides with that in (59) at convergence, while the derivatives $(\partial F/\partial \rho)_{Q,\varepsilon}$ and $(\partial F/\partial \varepsilon)_{Q,\rho}$ are analytically determined, as detailed in Appendix IV. Expressions (73) thus directly supply the partial derivatives

$$\left(\frac{\partial Y_3}{\partial \rho}\right)_\varepsilon, \quad \left(\frac{\partial Y_3}{\partial \varepsilon}\right)_\rho, \quad \left(\frac{\partial T}{\partial \rho}\right)_\varepsilon, \quad \left(\frac{\partial T}{\partial \varepsilon}\right)_\rho. \quad (74)$$

The analogous partial derivatives for $Y_i, i \neq 3$, are then determined using the exact partial derivatives of expressions (52) and (53), as detailed in Appendix V.

With these analytical developments the procedure for determining the Jacobian partial derivatives of pressure and temperature is theoretically complete. A practical implementation then utilizes expressions (70), (71) and (67)–(69) for numerical computations.

9. COMPUTATIONAL RESULTS

The procedure presented in the previous sections is specifically designed for coupling at each grid point the solution of the thermodynamic system (39)–(45) with Euler and Navier–Stokes CFD algorithms. For the purpose of documenting performance, the procedure has been used to generate the thermodynamic properties of equilibrium air by varying the density ρ and mass-specific internal energy ε over specified wide ranges corresponding to a temperature range of 8000 K and pressure range corresponding to a reference increase in altitude of over 30,000 m, i.e. 100,000 ft, above sea level. For direct comparison of results with independently published data, the computational predictions are then presented in sets of isobars, showing the variation of temperature versus inverse density and mass-specific internal energy and the distribution of the other thermodynamic variables versus temperature. The results are presented in terms of dimensional temperature, in degrees Kelvin, whereas the remaining thermodynamic variables are shown in non-dimensional form following expressions (30) in Section 5, with representative temperature, density and pressure set equal to the U.S. standard atmosphere values of these variables at sea level.

Figure 1 shows the variation of temperature versus inverse density, i.e. specific volume. Temperature is plotted versus specific volume $1/\rho$, because from the EOS in (7), temperature increases linearly with $1/\rho$ for a perfect gas. This convenient representation clearly shows, the difference between perfect and reacting air predictions. For a given density, hence specific volume, the chart illustrates the well-known incorrect high-temperature predictions of the perfect gas model, which become even more unrealistic as $1/\rho$, hence T , increases. As temperature increases further, the curves tend to approach straight lines, because at completion of the chemical reactions involved, the equilibrium air begins to behave for a certain range of temperature as a perfect gas of atomic oxygen and nitrogen. Overall, the temperature distributions in the figure remains continuous and smooth.

Another clear indication of the significant differences between perfect and reacting air behaviour is provided by Figure 2, which correlates with Figure 1 and presents the variation of temperature versus mass-specific internal energy. For low energies no chemical reactions occur, nor are the vibrational modes fully excited. Consequently, temperature remains independent of pressure and increases linearly with internal energy in this range. This correct trend follows the perfect gas TE in (7), which shows independence of pressure and a constant specific heat for the constant slope in the curve. Since temperature is a measure of the molecular kinetic energy mode,⁸ further increases in energy, accompanied by chemical reactions, reduce the rise in temperature in comparison with the perfect air case, because not all the internal energy corresponds to molecular kinetic energy. The larger ε , the greater is the discrepancy between perfect and reacting air predictions. As the graphs show, the rise in

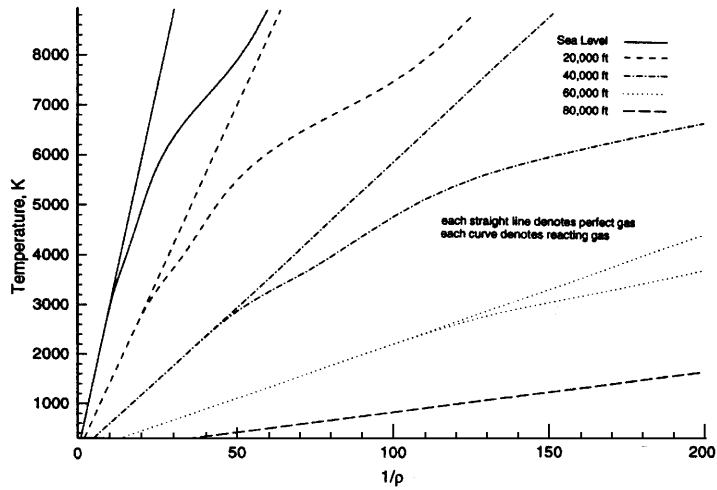


Fig. 1. Temperature versus $1/\rho$

temperature is further retarded by a decrease in pressure, which increases the rate of dissociations and thus further reduces the increase in molecular kinetic energy. For continuing increase of internal energy the curves then indicate a diminishing dependence on pressure and concurrent convergence towards a single straight line. This results from completion of the chemical reactions; hence the equilibrium air behaves for a certain range of energies as a perfect gas of atomic oxygen and nitrogen with pressure-independent constant specific heat, for the constant slope in the corresponding curve.

The distributions versus temperature of species mole fractions $X_i = (Y_i/M_i)/(\sum_{j=1}^5 Y_j/M_j)$ are presented in Figure 3.

At $p = 1$ atm the dissociation of molecular oxygen begins above 2000 K and is virtually complete above 4000 K; the dissociation of molecular nitrogen begins above 4000 K, when that of oxygen completes, and is virtually complete over 9000 K; nitric oxide begins to form at above 2000 K and its

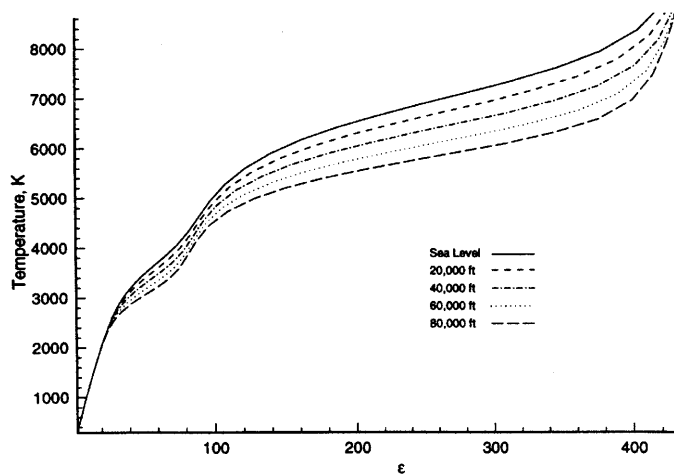


Fig. 2. Temperature versus ϵ

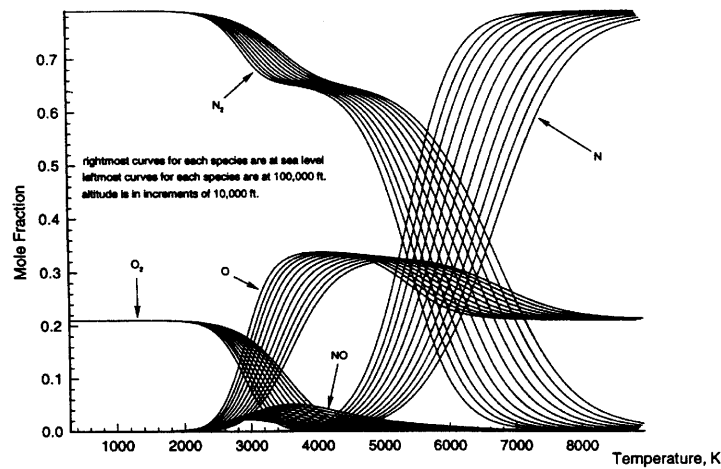


Fig. 3. Mole fractions versus temperature

mole fraction increases, reaches a peak at about 3500 K and then decreases. These features and all the $p = 1$ atm curves virtually coincide with the results reported in Reference 8. Furthermore, Reference 8 confirms the correctness of the qualitative shift of the mole fraction curves observed in the figure. A decrease in pressure favours dissociations; they can thus initiate at comparatively lower temperatures, which explains the shift to the left of the mole fraction curves. The observed decrease in oxygen and nitric oxide mole fractions, the ratio of species moles and mixture moles, is not so much due to a decrease in the number of atoms and molecules of these species, but rather to a drastic increase of the total number of mixture moles due to the rapid dissociation of molecular nitrogen. The results reported in Reference 10 then indicate that electrons and ionic species are virtually absent, since their mole fractions are less than 0.005 for $T < 8000$ K, which justifies the selection of a neutral reacting air model for this temperature range.

Figures 4 and 5 present the thermodynamic partial derivatives of temperature, $(\partial T/\partial \rho)_\varepsilon$ and $(\partial T/\partial \varepsilon)_\rho$, versus temperature. For low temperatures, $(\partial T/\partial \rho)_\varepsilon$ has to vanish, since temperature remains constant for fixed ε , according to the perfect air TE in (7). As temperature increases, the presence of chemical dissociations induces a strong dependence of T and $(\partial T/\partial \rho)_\varepsilon$ on ρ , because an increase in mixture density hampers dissociations and thus increases the molecular kinetic energy by an amount that for fixed ε would have been otherwise expended for the reactions. This effect is accentuated by a dissociation-favouring pressure decrease. As temperature increases further, however, the dependence of $(\partial T/\partial \rho)_\varepsilon$ on T rapidly decreases, because at completion of the chemical reactions the internal energy depends on temperature, but no longer on density, and for constant ε it follows that $(\partial T/\partial \rho)_\varepsilon \approx 0$ in these conditions.

The variation of $(\partial T/\partial \varepsilon)_\rho$ versus T directly correlates with the variation of T versus ε and mole fractions versus T . Even before chemical dissociations begin, this derivative is seen to decrease, as determined by the non-linear increase of the vibrational energy, which equals the translational kinetic energy at equilibrium. Therefore temperature, a measure of one mode of molecular energy among the translational, rotational and vibrational modes, increases less rapidly than ε , the sum of all the molecular energy modes. As the chemical reactions progress, they require increasing amounts of energy that will not be present as kinetic energy, hence $(\partial T/\partial \varepsilon)_\rho$ decreases further.

As the peak in nitric oxide mass fraction is reached, an increase in internal energy contributes to a proportional increase in molecular kinetic energy, which explains the increase in $(\partial T/\partial \varepsilon)_\rho$ until a

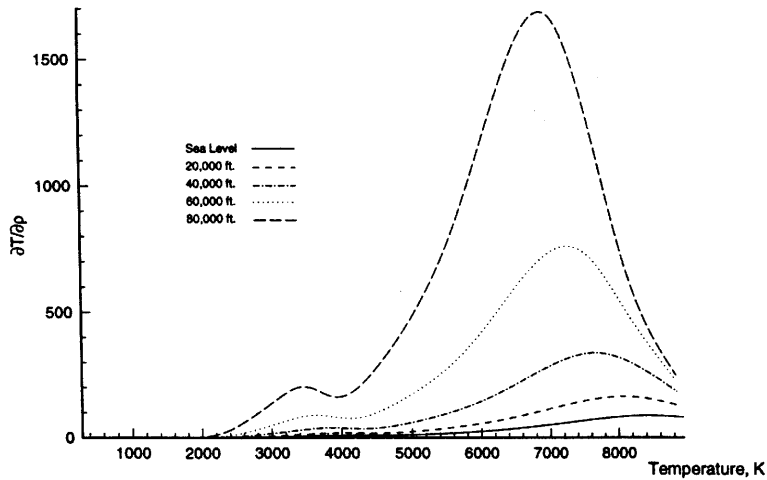


Fig. 4. $(\partial T/\partial \rho)_\epsilon$ versus temperature

state where a further increase in temperature initiates the dissociations of molecular nitrogen. This dissociation will then require increasing amounts of energy that will not be present as kinetic energy, hence $(\partial T/\partial \epsilon)_\rho$ begins to decrease again. As the chemical dissociations near completion, an increase in ϵ induces a proportional increase in molecular kinetic energy, which explains the renewed increase in $(\partial T/\partial \epsilon)_\rho$. A thermodynamic state is then reached where the reactions are complete, the mixture begins to behave as perfect air, within an appropriate range of T , and thus $(\partial T/\partial \epsilon)_\rho$ becomes equal to a constant, corresponding to the inverse of a specific heat. It is important to observe that for both derivatives the procedure generated smooth results.

Finally, Figures 6 and 7 present the variations of thermodynamic partial derivatives of pressure $(\partial p/\partial \rho)_\epsilon$ and $(\partial p/\partial \epsilon)_\rho$, versus temperature. The kinetic-theory interpretation of pressure as collisional variation of linear momentum⁸ explains these variations. Concerning the constant-density derivative

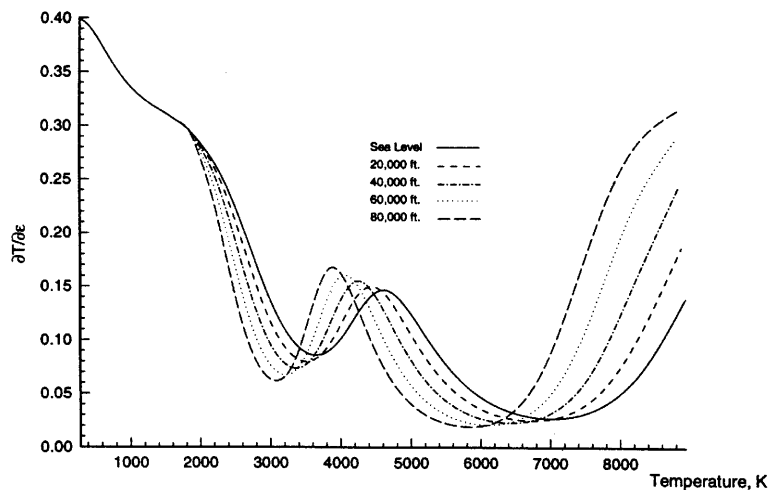


Fig. 5. $(\partial T/\partial \epsilon)_\rho$ versus temperature

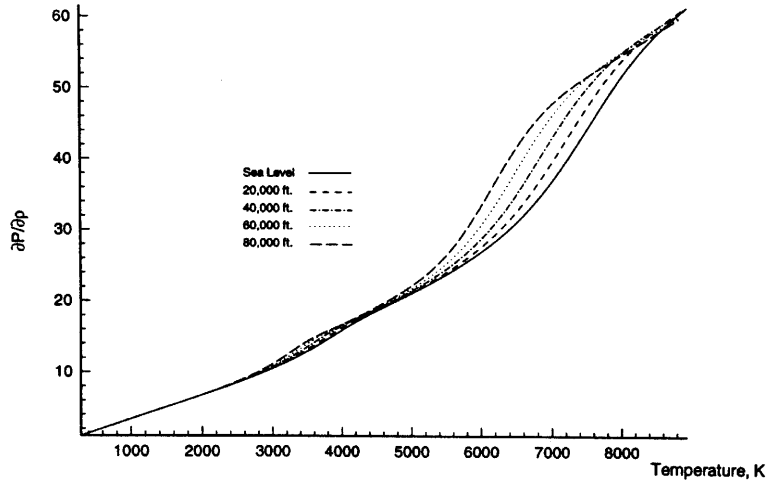


Fig. 6. $(\partial p / \partial \rho)_\epsilon$ versus temperature

$(\partial p / \partial \epsilon)_\rho$, as temperature increases and thus the chemical dissociations progress, the molecular kinetic energy, hence molecular linear momentum, will increase less rapidly than ϵ and consequently this thermodynamic derivative of pressure will decrease. For a fixed ϵ , conversely, as temperature increases and thus the chemical dissociations progress, an increase in mixture density corresponds to more species involved in collisions, which explains the increase in $(\partial p / \partial \rho)_\epsilon$. This thermodynamic derivatives varies linearly for low temperatures, because for a perfect gas, hence from (8), this derivative equals ϵ , which from (7) increases linearly with temperature. As temperature increases, the reacting air values of this derivative are greater than those for a perfect air, because the chemical reactions lead to more colliding species than in the perfect air case. For both derivatives a dissociation-favouring decrease in pressure then further reduces the increase in molecular kinetic energy and increases the number of colliding species, which explains the observed respective

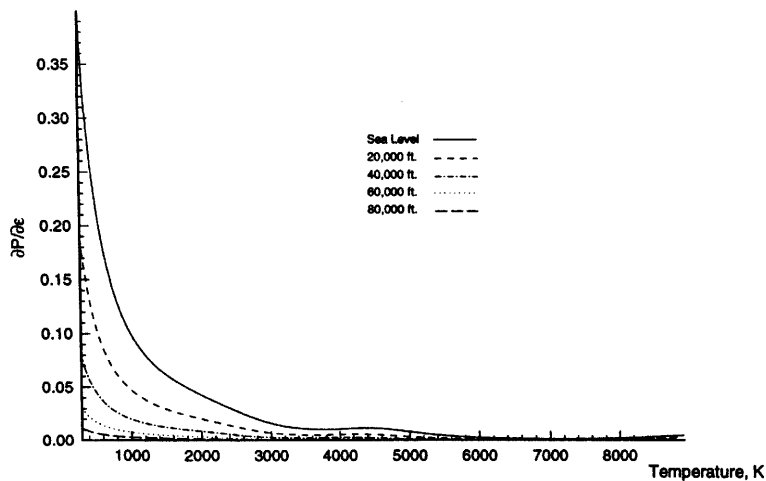


Fig. 7. $(\partial p / \partial \epsilon)_\rho$ versus temperature

variations of these derivatives with respect to pressure. Worthy of note also for these two derivatives is that the procedure generated smooth results.

10. CONCLUDING REMARKS

The procedure detailed in this paper directly generate pressure, temperature and mass and mole fractions as well as their thermodynamic and Jacobian partial derivatives for five-species neutral equilibrium air. Especially designed for explicit and implicit CFD algorithms, the procedure algebraically reduces the six-equation chemical equilibrium thermodynamic system and explicitly expresses four variables in terms of nitric oxide mass fraction and temperature. These two variables are then numerically determined by solving the internal energy and nitric oxide mass action equations through a Newton method solution, which is observed to converge in two to three iterations, for these two equations. The procedure then exactly determines the partial derivatives of pressure, temperature and mass fractions analytically.

All the computational results over a temperature range of 8000 K and pressure range corresponding to an increase in altitude of over 30,000 m (100,000 ft) above sea level are physically meaningful, while the predicted distributions of mole fractions for the model five species agree with independent published results. In particular, reference to the results in Reference 10 confirms that a neutral reacting air model remains accurate for temperatures below 8000 K. The thermodynamic properties so generated, including the important thermodynamic partial derivatives of pressure and temperature, are then observed to remain continuous and smooth. These results therefore support the procedure as an attractive alternative to incorporate the thermodynamic properties of reacting equilibrium air in Euler and Navier–Stokes CFD algorithms.

ACKNOWLEDGEMENTS

I wish to acknowledge the encouragement and interest of my colleague and mentor Dr. A. J. Baker, of the University of Tennessee, and the support of Dr. L. Povinelli, of ICOMP at the NASA Lewis Research Center, where initial notes on this procedure were revised. Dr. F. Zeleznik, also of NASA Lewis, provided interesting comments on an early draft of this paper. This work also benefited from the assistance of Alexy Kolesnikov and Mike Taylor, graduate students in our department, who generated the numerical results for Section 9. I am particularly grateful to Mike Taylor, who promptly and professionally generated the charts in this paper.

APPENDIX I: CHEMICAL AND THERMODYNAMICS PARAMETERS

The molecular masses for the chosen five species are⁹

$$\begin{aligned} M_1 &= 15.99940 \text{ kg kg-mol}^{-1}, \\ M_2 &= 14.00674 \text{ kg kg-mol}^{-1} \\ M_3 &= 30.00614 \text{ kg kg-mol}^{-1} \\ M_4 &= 31.99880 \text{ kg kg-mol}^{-1}, \\ M_5 &= 28.01348 \text{ kg kg-mol}^{-1}, \end{aligned} \tag{75}$$

where $M_3 = M_1 + M_2$, $M_4 = 2M_1$ and $M_5 = 2M_2$. In SI units the universal gas constant is

$$\mathcal{R} = 8314 \text{ J kg-mol}^{-1} \text{ K}^{-1}. \tag{76}$$

For the selected five species the thermodynamic parameters in (21) are expressed as^{7,8}

$$\theta_3^v = 2740 \text{ K}, \quad \theta_4^v = 2270 \text{ K}, \quad \theta_5^v = 3390 \text{ K}, \quad (77)$$

$$h_1^0 = 29,750 \frac{\mathcal{R}}{M_1} \text{ J kg}^{-1}, \quad h_2^0 = 56,500 \frac{\mathcal{R}}{M_2} \text{ J kg}^{-1}, \quad h_3^0 = 10,791.23871 \dots \frac{\mathcal{R}}{M_3} \text{ J kg}^{-1}. \quad (78)$$

Further, each c_{v_i} in (21) is determined as⁹

$$c_{v_1} = \frac{3}{2} \frac{\mathcal{R}}{M_1} \text{ J kg}^{-1} \text{ K}^{-1}, \quad c_{v_2} = \frac{3}{2} \frac{\mathcal{R}}{M_2} \text{ J kg}^{-1} \text{ K}^{-1},$$

$$c_{v_3} = \frac{5}{2} \frac{\mathcal{R}}{M_3} \text{ J kg}^{-1} \text{ K}^{-1}, \quad c_{v_4} = \frac{5}{2} \frac{\mathcal{R}}{M_4} \text{ J kg}^{-1} \text{ K}^{-1}, \quad c_{v_5} = \frac{5}{2} \frac{\mathcal{R}}{M_5} \text{ J kg}^{-1} \text{ K}^{-1}. \quad (79)$$

These expressions result from the kinetic theory of gases⁸ dictating that a monoatomic gas such as O possesses three independent energy absorption mechanisms (degrees of freedom) while a diatomic gas such as N₂ has five such degrees.

The internal energy equation (33) is simplified as

$$\tilde{\varepsilon} = \tilde{T} \sum_{i=1}^5 \left(c_{v_i} \frac{M_a}{\mathcal{R}} \right) Y_i + \sum_{i=3}^5 \frac{Y_i \left(\frac{\theta_i^v}{\gamma \mathcal{M}_r^2 T_\infty} \right) \frac{1}{M_i}}{\exp \left[\left(\frac{\theta_i^v}{\gamma \mathcal{M}_r^2 T_\infty} \right) \frac{1}{\tilde{T}} \right] - 1} + \sum_{i=1}^3 Y_i \tilde{h}_i^0. \quad (80)$$

The final form (34) is thus obtained by virtue of the expressions

$$\tilde{c}_{v_1} = \frac{3}{2} \frac{1}{\tilde{M}_1}, \quad \tilde{c}_{v_2} = \frac{3}{2} \frac{1}{\tilde{M}_2}, \quad \tilde{c}_{v_3} = \frac{5}{2} \frac{1}{\tilde{M}_3}, \quad \tilde{c}_{v_4} = \frac{5}{2} \frac{1}{\tilde{M}_4}, \quad \tilde{c}_{v_5} = \frac{5}{2} \frac{1}{\tilde{M}_5} \quad (81)$$

for each specific heat,

$$\tilde{\theta}_3^v = \frac{2740}{\gamma \mathcal{M}_r^2 T_\infty}, \quad \tilde{\theta}_4^v = \frac{2270}{\gamma \mathcal{M}_r^2 T_\infty}, \quad \tilde{\theta}_5^v = \frac{3390}{\gamma \mathcal{M}_r^2 T_\infty} \quad (82)$$

for each vibrational temperature and

$$\tilde{h}_1^0 = \frac{29,750}{\gamma \mathcal{M}_r^2 T_\infty \tilde{M}_1}, \quad \tilde{h}_2^0 = \frac{56,500}{\gamma \mathcal{M}_r^2 T_\infty \tilde{M}_2}, \quad \tilde{h}_3^0 = \frac{10,791.23871 \dots}{\gamma \mathcal{M}_r^2 T_\infty \tilde{M}_3} \quad (83)$$

for each formation enthalpy, which collectively indicates that (30) can significantly scale down these parameters.

APPENDIX II: CHEMICAL EQUILIBRIUM FUNCTIONS

While the procedure developed to solve system (39)–(45) is valid for arbitrary forms of equilibrium functions $K_i(T)$, $i = 1, 2, 3$, the numerical results presented in Section 9 were generated using the specific expressions of $K_i(T)$ reported in References 5 and 6. These expressions are

$$K_i(T) = \exp[A_1^i/Z + A_2^i + A_3^i \log(Z) + A_4^i Z + A_5^i Z^2], \quad i = 1, 2, \quad (84)$$

$$K_3(T) = \exp(A_1^i + A_2^i Z + A_3^i Z^2 + A_4^i Z^3 + A_5^i Z^4), \quad (85)$$

where $Z = 10,000/T$ and A_j^i are constant coefficients. Using an asymptotic analysis, the coefficients A_5^1 and A_5^3 have been slightly modified from those in References 5 and 6 to ensure a smooth

asymptotic convergence of the equilibrium air system (39)–(45) to either the perfect gas equation of state at lower temperatures or to the equation of state for an atomic-species gas mixture at higher temperatures. It was then observed that the difference between the equilibrium functions with original and modified coefficients remained negligible in the temperature range $600 \leq T \leq 8000$ K.

According to (26)–(28), asymptotic convergence is achieved if $K_i(T)$, $i = 1, 2, 3$, approach zero at lower temperatures, since Y_1, Y_2 and Y_3 vanish in this temperature range. Furthermore, $K_1(T)$ and $K_2(T)$ have to increase monotonically at higher temperatures, since Y_4 and Y_5 vanish at these temperatures. Conversely, $K_3(T)$ has to remain bounded at higher temperatures as a sufficient condition for attaining from (28) a vanishing Y_3 . The corresponding coefficients A_j^i for these equilibrium functions are given in Table I.

The equilibrium functions (84) and (85) are compactly expressed as

$$K_i(T) = \exp[F_i(T)]. \tag{86}$$

Consequently, the derivative of $K_i(T)$ with respect to T is cast as

$$\frac{dK_i(T)}{dT} = \exp[F_i(T)] \frac{dF_i(T)}{dT} = K_i \frac{dF_i}{dT}. \tag{87}$$

In (43)–(45) the non-dimensional equilibrium functions $\tilde{K}_i(\tilde{T})$ corresponding to (84) and (85) follow from inspection of (36)–(38) and directly depend upon \tilde{T} by expressing the variable Z in (84) and (85) as

$$Z = \frac{10,000}{T} = \left(\frac{10,000}{\gamma \mathcal{M}_T^2 T_\infty} \right) \left(\frac{\gamma \mathcal{M}_T^2 T_\infty}{T} \right) = \frac{\tilde{T}}{\tilde{T}}, \quad \tilde{T} = \frac{10,000}{\gamma \mathcal{M}_T^2 T_\infty}, \tag{88}$$

where \tilde{T} can be made substantially smaller than 10,000.

APPENDIX III. JACOBIAN DERIVATIVES FOR NEWTON'S ITERATION

The Jacobian partial derivatives (63)–(66) depend upon the four derivatives

$$\left(\frac{\partial Y_4}{\partial Y_3} \right)_{q,T}, \quad \left(\frac{\partial Y_4}{\partial T} \right)_{q,Y_3}, \quad \left(\frac{\partial Y_5}{\partial Y_3} \right)_{q,T}, \quad \left(\frac{\partial Y_5}{\partial T} \right)_{q,Y_3}, \tag{89}$$

which are directly computed using (52) and (53).

The partial derivative of (52) is

$$\left(\frac{\partial Y_4}{\partial Y_3} \right)_{q,T} = -\alpha_{13} + \frac{\alpha_{13} M_1^2 C_1}{2[M_1^2 C_1 (\alpha_{10} - \alpha_{13} Y_3 + M_1^2 C_1 / 4)]^{1/2}}. \tag{90}$$

The denominator is then re-expressed using (52) itself, yielding

$$\left(\frac{\partial Y_4}{\partial Y_3} \right)_{q,T} = -\alpha_{13} \left(1 + \frac{M_1^2 C_1}{2(Y_4 - \alpha_{10} + \alpha_{13} Y_3 - M_1^2 C_1 / 4)} \right). \tag{91}$$

Table I. Coefficients for equilibrium functions (84) and (85)

i	A_1^i	A_2^i	A_3^i	A_4^i	A_5^i
1	0.55388	9.367754721	1.77630	-6.5720	-0.031445
2	1.53510	8.513844721	1.29930	-11.4940	-0.006980
3	2.13500	-1.170000000	-0.38900	0.0610	-0.007000

Next (42) is inserted in the denominator, leading to

$$\left(\frac{\partial Y_4}{\partial Y_3}\right)_{q,T} = -\alpha_{13} \left(1 - \frac{M_1^2 C_1}{2Y_1 + M_1^2 C_1}\right) = -\frac{2\alpha_{13} Y_1}{2Y_1 + M_1^2 C_1}. \quad (92)$$

As a concluding step, $M_1^2 C_1$ is replaced by (43), yielding

$$\left(\frac{\partial Y_4}{\partial Y_3}\right)_{q,T} = -\frac{2\alpha_{13} Y_1 Y_4}{Y_1^2 + 2Y_1 Y_4} = -\frac{2\alpha_{13} Y_4}{Y_1 + 2Y_4}. \quad (93)$$

This simple expression only depends upon the mass fractions Y_1 and Y_4 and never becomes indeterminate, because the denominator remains constantly positive since Y_1 and Y_4 never vanish simultaneously. The partial derivative of Y_5 with respect to Y_3 is analogously determined as

$$\left(\frac{\partial Y_5}{\partial Y_3}\right)_{q,T} = -\frac{2\alpha_{23} Y_5}{Y_2 + 2Y_5}. \quad (94)$$

The same procedure is then employed to develop the partial derivative of Y_4 with respect to T as

$$\begin{aligned} \left(\frac{\partial Y_4}{\partial T}\right)_{q,Y_3} &= \frac{M_1^2}{2} \left(\frac{\partial C_1}{\partial T}\right)_\rho - \frac{M_1^2 C_1 (\alpha_{10} - \alpha_{13} Y_3 + M_1^2 C_1 / 2) dF_1 / dT}{2[M_1^2 C_1 (\alpha_{10} - \alpha_{13} Y_3 + M_1^2 C_1 / 4)]^{1/2}} \\ &= \frac{M_1^2 C_1}{2} \frac{dF_1}{dT} \left(1 - \frac{\alpha_{10} - \alpha_{13} Y_3 + M_1^2 C_1 / 2}{[M_1^2 C_1 (\alpha_{10} - \alpha_{13} Y_3 + M_1^2 C_1 / 4)]^{1/2}}\right) \\ &= \frac{M_1^2 C_1}{2} \frac{dF_1}{dT} \left(1 + \frac{Y_1 + Y_4 + M_1^2 C_1 / 2}{Y_4 - \alpha_{10} + \alpha_{13} Y_3 - M_1^2 C_1 / 2}\right) \\ &= \frac{M_1^2}{2} \frac{dF_1}{dT} \left(1 - \frac{Y_1 + Y_4 + M_1^2 C_1 / 2}{Y_1 + M_1^2 C_1 / 2}\right) \\ &= -\frac{M_1^2 C_1}{2} \frac{dF_1}{dT} \frac{Y_4}{Y_1 + M_1^2 C_1 / 2} \\ &= -\frac{Y_4}{[Y_1^2 / (2Y_4)] + 1} \frac{dF_1}{dT} \\ &= -\frac{Y_1 Y_4}{Y_1 + 2Y_4} \frac{dF_1}{dT}. \end{aligned} \quad (95)$$

The partial derivative of Y_5 with respect to T is analogously expressed as

$$\left(\frac{\partial Y_5}{\partial T}\right)_{q,Y_3} = -\frac{Y_2 Y_5}{Y_2 + 2Y_5} \frac{dF_2}{dT}. \quad (96)$$

These expressions are not indeterminate, since their denominator never vanishes. Using these expressions, the remaining mass fraction partial derivatives in (63)–(66),

$$\left(\frac{\partial Y_1}{\partial Y_3}\right)_{q,T}, \quad \left(\frac{\partial Y_1}{\partial T}\right)_{q,Y_3}, \quad \left(\frac{\partial Y_2}{\partial Y_3}\right)_{q,T}, \quad \left(\frac{\partial Y_2}{\partial T}\right)_{q,Y_3}, \quad (97)$$

are directly computed via (48) and (49) as

$$\left(\frac{\partial Y_1}{\partial Y_3}\right)_{q,T} = \left(\frac{\partial Y_1}{\partial Y_3}\right)_{Y_4} + \left(\frac{\partial Y_1}{\partial Y_4}\right)_{Y_3} \left(\frac{\partial Y_4}{\partial Y_3}\right)_{q,T} = -\alpha_{13} + \frac{2\alpha_{13}Y_4}{Y_1 + 2Y_4} = -\frac{\alpha_{13}Y_1}{Y_1 + 2Y_4}, \tag{98}$$

$$\left(\frac{\partial Y_1}{\partial T}\right)_{q,Y_3} = \left(\frac{\partial Y_1}{\partial Y_4}\right)_{Y_3} \left(\frac{\partial Y_4}{\partial T}\right)_{q,Y_3} = -\left(-\frac{Y_1Y_4}{Y_1 + 2Y_4}\right) \frac{dF_1}{dT} = \frac{Y_1Y_4}{Y_1 + 2Y_4} \frac{dF_1}{dT}, \tag{99}$$

$$\left(\frac{\partial Y_2}{\partial Y_3}\right)_{q,T} = \left(\frac{\partial Y_2}{\partial Y_3}\right)_{Y_5} + \left(\frac{\partial Y_2}{\partial Y_5}\right)_{Y_3} \left(\frac{\partial Y_5}{\partial Y_3}\right)_{q,T} = -\alpha_{23} + \frac{2\alpha_{23}Y_5}{Y_2 + 2Y_5} = -\frac{\alpha_{23}Y_2}{Y_2 + 2Y_5}, \tag{100}$$

$$\left(\frac{\partial Y_2}{\partial T}\right)_{q,Y_3} = \left(\frac{\partial Y_2}{\partial Y_5}\right)_{Y_3} \left(\frac{\partial Y_5}{\partial T}\right)_{q,Y_3} = -\left(-\frac{Y_2Y_5}{Y_2 + 2Y_5}\right) \frac{dF_2}{dT} = \frac{Y_2Y_5}{Y_2 + 2Y_5} \frac{dF_2}{dT}. \tag{101}$$

Further, the partial derivatives

$$\left(\frac{\partial f_1}{\partial Y_3}\right)_{q,Y_4,Y_5,T}, \quad \left(\frac{\partial f_1}{\partial Y_4}\right)_{q,Y_3,Y_5,T}, \quad \left(\frac{\partial f_1}{\partial Y_5}\right)_{q,Y_3,Y_4,T}, \quad \left(\frac{\partial f_1}{\partial T}\right)_{q,Y_3,Y_4,Y_5} \tag{102}$$

are determined from (56) as

$$\left(\frac{\partial f_1}{\partial Y_3}\right)_{q,Y_4,Y_5,T} = 1 \cdot 0, \tag{103}$$

$$\left(\frac{\partial f_1}{\partial Y_4}\right)_{q,Y_3,Y_5,T} = -\frac{M_3Y_5C_3}{2(Y_4Y_5C_3)^{1/2}} = -\frac{M_3(Y_4Y_5C_3)^{1/2}}{2Y_4} = -\frac{Y_3 - f_1}{2Y_4}, \tag{104}$$

$$\left(\frac{\partial f_1}{\partial Y_5}\right)_{q,Y_3,Y_4,T} = -\frac{M_3Y_4C_3}{2(Y_4Y_5C_3)^{1/2}} = -\frac{M_3(Y_4Y_5C_3)^{1/2}}{2Y_5} = -\frac{Y_3 - f_1}{2Y_5}, \tag{105}$$

$$\left(\frac{\partial f_1}{\partial T}\right)_{q,Y_3,Y_4,Y_5} = -\frac{M_3Y_4Y_5C_3}{2(Y_4Y_5C_3)^{1/2}} \frac{dF_3/dT}{2} = -\frac{M_3(Y_4Y_5C_3)^{1/2}}{2} \frac{dF_3}{dT} = -\frac{Y_3 - f_1}{2} \frac{dF_3}{dT}. \tag{106}$$

The partial derivatives

$$\left(\frac{\partial f_2}{\partial Y_3}\right)_{q,Y_1,Y_2,Y_4,Y_5,T}, \quad \left(\frac{\partial f_2}{\partial Y_1}\right)_{q,Y_3,Y_2,Y_4,Y_5,T}, \quad \left(\frac{\partial f_2}{\partial Y_2}\right)_{q,Y_3,Y_1,Y_4,Y_5,T}, \tag{107}$$

$$\left(\frac{\partial f_2}{\partial Y_4}\right)_{q,Y_3,Y_1,Y_2,Y_5,T}, \quad \left(\frac{\partial f_2}{\partial Y_5}\right)_{q,Y_3,Y_1,Y_2,Y_4,T}, \quad \left(\frac{\partial f_2}{\partial T}\right)_{q,Y_3,Y_1,Y_2,Y_4,Y_5} \tag{108}$$

are then determined from (57) as

$$\left(\frac{\partial f_2}{\partial Y_3}\right)_{q, Y_1, Y_2, Y_4, Y_5, T} = -Tc_{v_3} - \frac{\theta_3^v/M_3}{\exp(\theta_3^v/T) - 1} - h_3^0, \quad (109)$$

$$\left(\frac{\partial f_2}{\partial Y_1}\right)_{q, Y_3, Y_2, Y_4, Y_5, T} = -Tc_{v_1} - h_1^0, \quad (110)$$

$$\left(\frac{\partial f_2}{\partial Y_2}\right)_{q, Y_3, Y_1, Y_4, Y_5, T} = -Tc_{v_2} - h_2^0, \quad (111)$$

$$\left(\frac{\partial f_2}{\partial Y_4}\right)_{q, Y_3, Y_1, Y_2, Y_5, T} = -Tc_{v_4} - \frac{\theta_4^v/M_4}{\exp(\theta_4^v/T) - 1}, \quad (112)$$

$$\left(\frac{\partial f_2}{\partial Y_5}\right)_{q, Y_3, Y_1, Y_2, Y_4, T} = -Tc_{v_5} - \frac{\theta_5^v/M_5}{\exp(\theta_5^v/T) - 1}, \quad (113)$$

$$\left(\frac{\partial f_2}{\partial T}\right)_{q, Y_3, Y_1, Y_2, Y_4, Y_5} = -\sum_{i=1}^5 c_{v_i} Y_i - \sum_{i=3}^5 \frac{Y_i(\theta_i^v/M_i)(\theta_i^v/T^2) \exp(\theta_i^v/T)}{[\exp(\theta_i^v/T) - 1]^2}. \quad (114)$$

Consequently, the expressions for the partial derivatives (63)–(66) of f_1 and f_2 with respect to Y_3 and T are

$$\left(\frac{\partial f_1}{\partial Y_3}\right)_{q, T} = 1 + (Y_3 - f_1) \left(\frac{\alpha_{13}}{Y_1 + 2Y_4} + \frac{\alpha_{23}}{Y_2 + 2Y_5} \right), \quad (115)$$

$$\left(\frac{\partial f_1}{\partial T}\right)_{q, Y_3} = \frac{Y_3 - f_1}{2} \left(\frac{Y_1}{Y_1 + 2Y_4} \frac{dF_1}{dT} + \frac{Y_2}{Y_2 + 2Y_5} \frac{dF_2}{dT} - \frac{dF_3}{dT} \right), \quad (116)$$

$$\begin{aligned} \left(\frac{\partial f_2}{\partial Y_3}\right)_{q, T} &= -Tc_{v_3} - \frac{\theta_3^v/M_3}{\exp(\theta_3^v/T) - 1} - h_3^0 + (Tc_{v_1} + h_1^0) \frac{\alpha_{13} Y_1}{Y_1 + 2Y_4} + (Tc_{v_2} + h_2^0) \frac{\alpha_{23} Y_2}{Y_2 + 2Y_5} \\ &+ \left(Tc_{v_4} + \frac{\theta_4^v/M_4}{\exp(\theta_4^v/T) - 1} \right) \frac{2\alpha_{13} Y_4}{Y_1 + 2Y_4} + \left(Tc_{v_5} + \frac{\theta_5^v/M_5}{\exp(\theta_5^v/T) - 1} \right) \frac{2\alpha_{23} Y_5}{Y_2 + 2Y_5}, \end{aligned} \quad (117)$$

$$\begin{aligned} \left(\frac{\partial f_2}{\partial T}\right)_{q, Y_3} &= -\sum_{i=1}^5 c_{v_i} Y_i - \sum_{i=3}^5 \frac{Y_i(\theta_i^v/M_i)(\theta_i^v/T^2) \exp(\theta_i^v/T)}{[\exp(\theta_i^v/T) - 1]^2} - (Tc_{v_1} + h_1^0) \frac{Y_1 Y_4}{Y_1 + 2Y_4} \frac{dF_1}{dT} \\ &- (Tc_{v_2} + h_2^0) \frac{Y_2 Y_5}{Y_2 + 2Y_5} \frac{dF_2}{dT} \\ &+ \left(Tc_{v_4} + \frac{\theta_4^v/M_4}{\exp(\theta_4^v/T) - 1} \right) \frac{Y_1 Y_4}{Y_1 + 2Y_4} \frac{dF_1}{dT} + \left(Tc_{v_5} + \frac{\theta_5^v/M_5}{\exp(\theta_5^v/T) - 1} \right) \frac{Y_2 Y_5}{Y_2 + 2Y_5} \frac{dF_2}{dT}. \end{aligned} \quad (118)$$

APPENDIX IV: PARTIAL DERIVATIVES OF f_1 AND f_2 WITH RESPECT TO ρ AND ε

The partial derivatives in (98),

$$\left(\frac{\partial F}{\partial \rho}\right)_{Q,\varepsilon}, \quad \left(\frac{\partial F}{\partial \varepsilon}\right)_{Q,\rho},$$

are expressed as

$$\left(\frac{\partial f_1}{\partial \rho}\right)_{Y_3,T,\varepsilon} = \left(\frac{\partial f_1}{\partial Y_4}\right)_{q,Y_3,Y_5,T} \left(\frac{\partial Y_4}{\partial \rho}\right)_{Y_3,T} + \left(\frac{\partial f_1}{\partial Y_5}\right)_{q,Y_3,Y_4,T} \left(\frac{\partial Y_5}{\partial \rho}\right)_{Y_3,T}, \tag{119}$$

$$\left(\frac{\partial f_1}{\partial \varepsilon}\right)_{Y_3,T,\rho} = 0.0, \tag{120}$$

$$\begin{aligned} \left(\frac{\partial f_2}{\partial \rho}\right)_{Y_3,T,\varepsilon} &= \left(\frac{\partial f_2}{\partial Y_1}\right)_{q,Y_2,Y_3,Y_4,Y_5,T} \left(\frac{\partial Y_1}{\partial \rho}\right)_{Y_3,T} + \left(\frac{\partial f_2}{\partial Y_2}\right)_{q,Y_1,Y_3,Y_4,Y_5,T} \left(\frac{\partial Y_2}{\partial \rho}\right)_{Y_3,T} \\ &+ \left(\frac{\partial f_2}{\partial Y_4}\right)_{q,Y_1,Y_2,Y_3,Y_5,T} \left(\frac{\partial Y_4}{\partial \rho}\right)_{Y_3,T} + \left(\frac{\partial f_2}{\partial Y_5}\right)_{q,Y_1,Y_2,Y_3,Y_4,T} \left(\frac{\partial Y_5}{\partial \rho}\right)_{Y_3,T}, \end{aligned} \tag{121}$$

$$\left(\frac{\partial f_2}{\partial \varepsilon}\right)_{Y_3,T,\rho} = \left(\frac{\partial f_2}{\partial \varepsilon}\right)_{Y_1,Y_2,Y_3,Y_4,Y_5,T,\rho} = 1.0. \tag{122}$$

These expressions depend on the partial derivatives

$$\left(\frac{\partial f_1}{\partial Y_i}\right)_{q,Y_j,T}, \quad \left(\frac{\partial f_2}{\partial Y_i}\right)_{q,Y_j,T}, \quad i \neq j, \tag{123}$$

$$\left(\frac{\partial Y_4}{\partial \rho}\right)_{Y_3,T}, \quad \left(\frac{\partial Y_5}{\partial \rho}\right)_{Y_3,T}, \quad \left(\frac{\partial Y_1}{\partial \rho}\right)_{Y_3,T}, \quad \left(\frac{\partial Y_2}{\partial \rho}\right)_{Y_3,T}. \tag{124}$$

Expressions (123) are presented in Appendix III, while expressions (124) are determined through a procedure similar to that in (90) as follows. From (52) the partial derivative of Y_4 with respect to ρ is

$$\begin{aligned} \left(\frac{\partial Y_4}{\partial \rho}\right)_{Y_3,T} &= \frac{M_1^2}{2} \left(\frac{\partial C_1}{\partial \rho}\right)_T - \frac{M_1^2(\alpha_{10} - \alpha_{13}Y_3 + M_1^2C_1/2)(\partial C_1/\partial \rho)_T}{2[M_1^2C_1(\alpha_{10} - \alpha_{13}Y_3 + M_1^2C_1/4)]^{1/2}} \\ &= -\frac{M_1^2C_1}{2\rho} - \frac{(M_1^2C_1/\rho)(\alpha_{10} - \alpha_{13}Y_3 + M_1^2C_1/2)}{2(Y_4 - \alpha_{10} + \alpha_{13}Y_3 - M_1^2C_1/2)} \\ &= -\frac{M_1^2C_1}{2\rho} \left(1 + \frac{Y_1 + Y_4 + M_1^2C_1/2}{Y_4 - \alpha_{10} + \alpha_{13}Y_3 - M_1^2C_1/2}\right) \\ &= \frac{M_1^2C_1}{2\rho} \frac{Y_4}{Y_1 + M_1^2C_1/2} \\ &= \frac{1}{\rho} \frac{Y_4}{Y_1/[Y_1^2/(2Y_4)] + 1} \\ &= \frac{Y_1Y_4}{Y_1 + 2Y_4\rho}. \end{aligned} \tag{125}$$

The partial derivative of Y_5 with respect to ρ is analogously expressed as

$$\left(\frac{\partial Y_5}{\partial \rho}\right)_{Y_3, T} = \frac{Y_2 Y_5}{Y_2 + 2Y_5} \frac{1}{\rho}. \quad (126)$$

The partial derivatives of Y_1 and Y_2 directly follow from (48) and (49) as

$$\left(\frac{\partial Y_1}{\partial \rho}\right)_{Y_3, T} = -\frac{Y_1 Y_4}{Y_1 + 2Y_4} \frac{1}{\rho}, \quad \left(\frac{\partial Y_2}{\partial \rho}\right)_{Y_3, T} = -\frac{Y_2 Y_5}{Y_2 + 2Y_5} \frac{1}{\rho}. \quad (127)$$

With these expressions the partial derivatives (119)–(122) become

$$\left(\frac{\partial f_1}{\partial \rho}\right)_{Y_3, T, \varepsilon} = -\frac{1}{2\rho} \frac{Y_1 Y_3}{Y_1 + 2Y_4} - \frac{1}{2\rho} \frac{Y_2 Y_3}{Y_2 + 2Y_5}, \quad (128)$$

$$\left(\frac{\partial f_1}{\partial \varepsilon}\right)_{Y_3, T, \rho} = 0.0, \quad (129)$$

$$\begin{aligned} \left(\frac{\partial f_2}{\partial \rho}\right)_{Y_3, T, \varepsilon} &= (Tc_{v_1} + h_1^0) \frac{1}{\rho} \frac{Y_1 Y_4}{Y_1 + 2Y_4} + (Tc_{v_2} + h_2^0) \frac{1}{\rho} \frac{Y_2 Y_5}{Y_2 + 2Y_5} \\ &\quad - \left(Tc_{v_4} + \frac{\theta_4^v/M_4}{\exp(\theta_4^v/T) - 1}\right) \frac{1}{\rho} \frac{Y_1 Y_4}{Y_1 + 2Y_4} - \left(Tc_{v_5} + \frac{\theta_5^v/M_5}{\exp(\theta_5^v/T) - 1}\right) \frac{1}{\rho} \frac{Y_2 Y_5}{Y_2 + 2Y_5}, \end{aligned} \quad (130)$$

$$\left(\frac{\partial f_2}{\partial \varepsilon}\right)_{Y_3, T, \rho} = 1.0. \quad (131)$$

APPENDIX V: PARTIAL DERIVATIVES OF Y_1, Y_2, Y_4 AND Y_5 WITH RESPECT TO ρ AND ε

The thermodynamic partial derivatives of pressure, (70) and (71), depend on the partial derivatives

$$\left(\frac{\partial Y_4}{\partial \rho}\right)_\varepsilon, \quad \left(\frac{\partial Y_4}{\partial \varepsilon}\right)_\rho, \quad \left(\frac{\partial Y_5}{\partial \rho}\right)_\varepsilon, \quad \left(\frac{\partial Y_5}{\partial \varepsilon}\right)_\rho. \quad (132)$$

Given the functional relations (54) and (55) for $Y_i, i \neq 3$, these derivatives are expressed as

$$\left(\frac{\partial Y_4}{\partial \rho}\right)_\varepsilon = \left(\frac{\partial Y_4}{\partial Y_3}\right)_{\rho, T} \left(\frac{\partial Y_3}{\partial \rho}\right)_\varepsilon + \left(\frac{\partial Y_4}{\partial T}\right)_{\rho, Y_3} \left(\frac{\partial T}{\partial \rho}\right)_\varepsilon + \left(\frac{\partial Y_4}{\partial \rho}\right)_{Y_3, T}, \quad (133)$$

$$\left(\frac{\partial Y_4}{\partial \varepsilon}\right)_\rho = \left(\frac{\partial Y_4}{\partial Y_3}\right)_{\rho, T} \left(\frac{\partial Y_3}{\partial \varepsilon}\right)_\rho + \left(\frac{\partial Y_4}{\partial T}\right)_{\rho, Y_3} \left(\frac{\partial T}{\partial \varepsilon}\right)_\rho, \quad (134)$$

$$\left(\frac{\partial Y_5}{\partial \rho}\right)_\varepsilon = \left(\frac{\partial Y_5}{\partial Y_3}\right)_{\rho, T} \left(\frac{\partial Y_3}{\partial \rho}\right)_\varepsilon + \left(\frac{\partial Y_5}{\partial T}\right)_{\rho, Y_3} \left(\frac{\partial T}{\partial \rho}\right)_\varepsilon + \left(\frac{\partial Y_5}{\partial \rho}\right)_{Y_3, T}, \quad (135)$$

$$\left(\frac{\partial Y_5}{\partial \varepsilon}\right)_\rho = \left(\frac{\partial Y_5}{\partial Y_3}\right)_{\rho, T} \left(\frac{\partial Y_3}{\partial \varepsilon}\right)_\rho + \left(\frac{\partial Y_5}{\partial T}\right)_{\rho, Y_3} \left(\frac{\partial T}{\partial \varepsilon}\right)_\rho, \quad (136)$$

where the partial derivatives of Y_4 and Y_5 with respect to Y_3 and T are detailed in Appendix III. Hence expressions (133)–(136) are cast as

$$\left(\frac{\partial Y_4}{\partial \rho}\right)_\varepsilon = -\frac{2\alpha_{13}Y_4}{Y_1+2Y_4}\left(\frac{\partial Y_3}{\partial \rho}\right)_\varepsilon - \frac{Y_1Y_4}{Y_1+2Y_4}\frac{dF_1}{dT}\left(\frac{\partial T}{\partial \rho}\right)_\varepsilon + \frac{Y_1Y_4}{Y_1+2Y_4}\frac{1}{\rho}, \quad (137)$$

$$\left(\frac{\partial Y_4}{\partial \varepsilon}\right)_\rho = -\frac{2\alpha_{13}Y_4}{Y_1+2Y_4}\left(\frac{\partial Y_3}{\partial \varepsilon}\right)_\rho - \frac{Y_1Y_4}{Y_1+2Y_4}\frac{dF_1}{dT}\left(\frac{\partial T}{\partial \varepsilon}\right)_\rho, \quad (138)$$

$$\left(\frac{\partial Y_5}{\partial \rho}\right)_\varepsilon = -\frac{2\alpha_{23}Y_5}{Y_2+2Y_5}\left(\frac{\partial Y_3}{\partial \rho}\right)_\varepsilon - \frac{Y_2Y_5}{Y_2+2Y_5}\frac{dF_2}{dT}\left(\frac{\partial T}{\partial \rho}\right)_\varepsilon + \frac{Y_2Y_5}{Y_2+2Y_5}\frac{1}{\rho}, \quad (139)$$

$$\left(\frac{\partial Y_5}{\partial \varepsilon}\right)_\rho = -\frac{2\alpha_{23}Y_5}{Y_2+2Y_5}\left(\frac{\partial Y_3}{\partial \varepsilon}\right)_\rho - \frac{Y_2Y_5}{Y_2+2Y_5}\frac{dF_2}{dT}\left(\frac{\partial T}{\partial \varepsilon}\right)_\rho. \quad (140)$$

With these expressions and using (48) and (49), the partial derivatives

$$\left(\frac{\partial Y_1}{\partial \rho}\right)_\varepsilon, \quad \left(\frac{\partial Y_1}{\partial \varepsilon}\right)_\rho, \quad \left(\frac{\partial Y_2}{\partial \rho}\right)_\varepsilon, \quad \left(\frac{\partial Y_2}{\partial \varepsilon}\right)_\rho \quad (141)$$

are developed as

$$\left(\frac{\partial Y_1}{\partial \rho}\right)_\varepsilon = -\left(\frac{\partial Y_4}{\partial \rho}\right)_\varepsilon - \alpha_{13}\left(\frac{\partial Y_3}{\partial \rho}\right)_\varepsilon, \quad (142)$$

$$\left(\frac{\partial Y_1}{\partial \varepsilon}\right)_\rho = -\left(\frac{\partial Y_4}{\partial \varepsilon}\right)_\rho - \alpha_{13}\left(\frac{\partial Y_3}{\partial \varepsilon}\right)_\rho, \quad (143)$$

$$\left(\frac{\partial Y_2}{\partial \rho}\right)_\varepsilon = -\left(\frac{\partial Y_5}{\partial \rho}\right)_\varepsilon - \alpha_{23}\left(\frac{\partial Y_3}{\partial \rho}\right)_\varepsilon, \quad (144)$$

$$\left(\frac{\partial Y_2}{\partial \varepsilon}\right)_\rho = -\left(\frac{\partial Y_5}{\partial \varepsilon}\right)_\rho - \alpha_{23}\left(\frac{\partial Y_3}{\partial \varepsilon}\right)_\rho. \quad (145)$$

REFERENCES

1. J. C. Tannehil and P. H. Mugge, 'Improved curve fits for the thermodynamic properties of equilibrium air suitable for numerical computation using time-dependent or shock-capturing methods, *NASA CR-2470*, 1974.
2. M. S. Liou, B. van Leer and J. S. Shuen, 'Splitting of inviscid fluxes for real gases', *J. Comput. Phys.*, **87**, 1–24 (1990).
3. R. K. Prabhu, J. R. Stewart and R. R. Thareja, 'A Navier–Stokes solver for high speed equilibrium flows and application to blunt bodies', *AIAA Paper 89-0668*, 1989.
4. H. C. Yee, G. H. Klopfer and J. L. Montagne, 'High resolution shock-capturing schemes for inviscid and viscous hypersonic flows', *J. Comput. Phys.*, **88**, 31–61 (1990).
5. C. Park, 'On convergence of computation of chemically reacting flows', *AIAA Paper 85-0247*, 1985.
6. C. Park and S. Yoon, 'A fully-coupled implicit method for thermo-chemical non-equilibrium air at sub-orbital flight speeds', *AIAA Paper 89-1974*, 1989.
7. J.-A. Desideri, N. Glinsky and E. Hettner, 'Hypersonic reacting flow computations', *Comput. Fluids*, **18**, 151–182 (1990).
8. J. D. Anderson, Jr., *Hypersonic and High Temperature Gas Dynamics*, McGraw-Hill, New York, 1989.
9. W. G. Vincenti and C. H. Kruger, *Introduction to Physical Gasdynamics*, Wiley, New York, 1965.
10. M. Rasmussen, *Hypersonic Flow*, Wiley, New York, 1994.
11. K. Meintjes and A. P. Morgan, 'Element variables and the solution of complex chemical equilibrium problems', *Combust. Sci. Technol.*, **68**, 35–48 (1989).